Investigation of circulating microRNAs in response to transcatheter aortic valve replacement and exploration of their cellular function in cardiovascular cells

Inaugural-Dissertation

zur Erlangung des Doktorgrades

der Hohen Medizinischen Fakultät

der Rheinischen Friedrich-Wilhelms-Universität

Bonn

Xiang Xu

aus Qingdao/China

2021

Angefertigt mit der Genehmigung

der Medizinischen Fakultät der Universität Bonn

1. Gutachter: PD Dr. med. Felix Jansen
2. Gutachter: Prof. Dr. Zeinad Abdullah

Tag der Mündlichen Prüfung: 04.05.2021

Aus der Medizinischen Klinik II - Innere Medizin (Kardiologie, Pneumologie)

Direktor: Prof. Dr. med. Georg Nickenig

Table of Contents

List of abbreviations

7-AAD	7-aminoactinomycin
ACS	acute coronary syndrome
AS	aortic stenosis
Bcl-2	b-cell lymphoma 2
BIRC8	baculoviral IAP repeat-containing protein 8
CMs	cardiac myocytes
CVD	cardiovascular disease
DAPI	4′,6-diamidino 2phenylindole
ECs	endothelial cells
EVs	extracellular vesicles
FCs	fibroblast cells
H_2O_2	hydrogen peroxide
LVEF	left ventricular ejection fraction
miRs	microRNAs
MVs	microvesicles
NAIP	baculoviral IAP repeat-containing protein 1
NOD2	nucleotide-binding oligomerization domain-containing protein 2
SAVR	surgical aortic valve replacement
TAVR	transcatheter aortic valve replacement

1. Introduction

1.1 Aortic stenosis, heart failure, and transcatheter aortic valve replacement

Aortic stenosis (AS) is one of the most frequent degenerative valvular heart diseases and its prevalence is increasing with the aging of the population. It is characterized by continuous calcification of the matrix, progressive fibrosis, consequent increases in valve stiffness, and therefore narrowing of aortic valve opening. Aortic stenosis restricts the blood outflow from the left ventricle to aorta and increases left ventricular afterload. The overload of left ventricular pressure results in two different but overlapping processes. The first stage is concentric left ventricular hypertrophy and increased wall thickness, which is caused by the AS-induced pressure overload (Badeer, 1964, Carabello, et al., 2009). The second stage is characterized by myocardial fibrosis, apoptosis, reduced ventricular compliance, and diastolic dysfunction (Villari, et al., 1995, Hein, et al., 2003). Once the on-going left ventricular dysfunction fails to be relieved, irreversible pathological changes of myocardium will occur, which lead to reduced left ventricular ejection fraction and heart failure.

Heart failure is a compex pathophysiological process that is affected by many different bioactive molecules. An increased level of oxidative stress is one of the most commonly suggested mechanisms to affect heart function. Reactive oxygen species (ROS) can induce most of the changes that contribute to impaired heart function, such as myocyte hypertrophy, apoptosis and abnormal matrix changes (Sawyer, et al., 2002). Therefore, oxidative stress plays an important role in the pathogenesis of heart failure and remodelling. As the stenosis progresses, main symptoms such as angina, dyspnea, and dizziness/syncope occur in some of AS patients. Surgical aortic valve replacement (SAVR) was the only effective treatment for many years and is still the better option for some patients. However, recently, considering the high risk and complications of open-heart surgery, transcatheter aortic valve replacement (TAVR) has emerged as an alternative interventional treatment and gradually become the standard treatment for some patients with severe symptomatic AS. Encouraging data from large randomized controlled trials show that TAVR is equally effective compared with SAVR (Thyregod, et

al., 2019, Gleason, et al., 2018). Clinical assessment of several hemodynamic parameters such as velocity, gradients, and aortic valve area additionally help the classification and accurate treatment of this disease (Nishimura, et al., 2018). However, even in patients who meet the criteria for TAVR, some of them still do not derive hemodynamic improvement or anticipated survival benefit from TAVR (Howard, et al., 2014).

1.2 Intercellular communication within the heart

The heart consists of different cell types like cardiac myocytes (CMs), endothelial cells (ECs), fibroblasts, stem cells, and inflammatory cells (Segers, et al., 2008). CMs are contractile cells containing numerous mitochondria which provide energy needed to allow conduction and contraction of cells. By this feature, they carry out mechanical and electrical functions which are most essential to support pumping of heart. Fibroblasts maintain the structural integrity of heart and play a vital role in wound closure and repair. Endothelial cells, which outnumber all other cell types in the heart, comprise more than 60% of the non-cardiomyocyte cells in heart (Pinto, et al., 2016) . They have complex biological functions, including the control of vascular permeability, regulation of hemostasis and angiogenesis. In addition to various cells residing in heart, the extracellular matrix (ECM) is also a complex network consisting of different proteins and contribute to the cross-talk. The ECM is able to store and release different growth factors, chemokines and cytokines that modulate cell functions. For example, cytokines such as interleukin-6 can stimulate the production of growth factors transforming growth factor beta (TGF-β) and Vascular endothelial growth factor (VEGF) which increase proliferation of cells and myofibroblast differentiation. They play key roles in angiogenesis and cardiac hypertrophy (Fearon, et al., 1999, Midgley, et al., 2013). In addition to the interaction between cells and ECM, cells in the heart can communicate with each other through multiple ways including chemical, mechanical and electrical signaling. Secretion of miR-21 in exosomes from fibroblast has been shown to induce cardiomyocyte hypertrophy (Bang, et al., 2014). TGF-β–activated myofibroblasts exert tonic contractile forces on myocytes and slow electric conduction by channel activation (Thompson, et al., 2011). A number of studies also demonstrated the interaction between fibroblast and endothelial cells. Fibroblast secreted growth factors (FGF) and vascular endothelial growth factor

(VEGF) are strong inducers which act on endothelial cells and stimulate angiogenesis, while VEGF-induced tube formation in vitro can be inhibited by the expression of pigment epithelium-derived growth factor (PEDF) from cardiac fibroblasts (Howard, et al., 2014, Rychli, et al., 2010). Moreover, the fibroblasts-secreted matrix metalloproteinases (MMPs) and tissue inhibitor of metalloproteinases (TIMPs) are also involved in angiogenesis by promotion or inhibition of tube formation (Lambert, et al., 2004). Because of the abundance of ECs and the important function of myocytes in the heart, the communication between these two types of cells is of great importance for the heart. ECs can secrete small molecules such as Nitric oxide (NO) to modulate cardiac contractility and remodelling. Endothelial dysfunction leads to decreased NO production and protein kinase G (PKG) activity in adjacent CMs, which result in hypertrophy and stiffness of the heart (Paulus et al., 2013). Studies have also shown that the expression of endothelium-derived proteins, such as interleukin-6, periostin, and thrombospondin can increase in ECs in response to pressure overload. These proteins affect target myocytes and regulate cardiac remodelling (Vincent, et al., 2018). Recently, an increasing number of studies have been focused on the effect of extracellular vesicles on cell-to-cell communication (Figure 1). Tumour Necrosis Factor-alpha (TNF-α) is not produced under normal conditions in the heart, but it is packaged into extracellular vesicles (EVs) from cardiomyocytes under stress conditions and thereby induces apoptosis in neighbouring cardiomyocytes (Yu, et al., 2012).

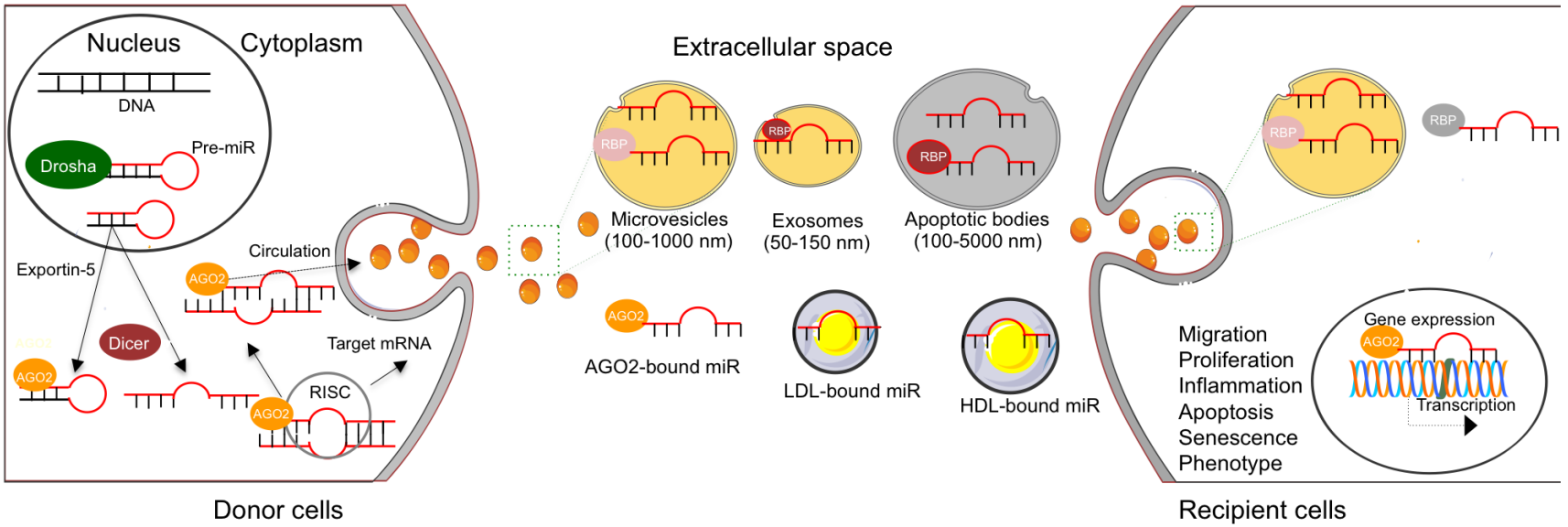

Fig. 1: Schematic diagram of the biogenesis and transfer of microRNAs into target cells via extracellular vesicles. MiRs are transcribed in the nucleus and subjected to sequential enzymatic processing steps. In the cytoplasm, mature miRNAs can be incorporated and released by extracellular vesicles or in a complex with molecules such as argonaute proteins (AGO2), low-density lipoproteins (LDL), or high-density lipoproteins (HDL). (Modified from Hosen MR., et al., 2020)

1.3 Circulating microRNA and extracellular vesicles in cardiovascular disease.

EVs are small membrane vesicles secreted by cells into the extracellular space. Based on the differences in their size, content, biogenesis and release pathways, EVs can be classified into three subtypes: microvesicles (MVs), exosomes, and apoptotic bodies. The contents of cargos within include lipids, nucleic acids and proteins. Originally, EVs were thought to be unwanted cellular wastes. However, it has since been determined that they are important carriers of bioactive molecules and play essential roles in cell-cell communication between local or distant cells (Zaborowski, et al., 2015). These vesicles may originate from the local cells but may also come from a distant location via the circulating blood supply. Once released into the bloodstream, EVs can interact with local CMs, ECs, fibroblasts, and immune cells to participate in either cardiac damage or repair. For example, by transferring microRNAs (miRs) contained inside the vesicle to a recipient cell, EVs could modulate the function of target endothelial cells or cadiomyocytes and further influence the progression of the disease (Gan, et al., 2020, Liu, et al., 2019). Moreover, EVs can promote vascular endothelial repair by delivering functional miR-126 into recipient cells (Jansen, et al., 2013). Recently, a newly pubished article summarized and reported that exosomes, the small EV that have long been offered as a promising drug delivery system for small molecules in basic scientific research, are now in the clinic (Cully M, 2020). For example, a phase I clinical trial using RASG12D siRNA-containing exosomes to target RAS, run by MD Anderson, is set to start shortly. This is based on the findings showing that RASG12D siRNA-containing exosomes improved survival in a model of pancreatic cancer because G12D mutant is often found in pancreatic cancer and pancreas is particularly good at taking up intravenously delivered exosomes. Moreover, Codiak Biosciences, the company which is the first to start a human trial of an engineered exosome-based therapeutic, have launched a phase I/II clinical trial in october using the engineered exosome to treat advanced solid tumours. As a novel platform, exosomes face not only scientific but also practical challenges. However, it will provide us new opportunities and might be the effective vector in clinical practice.

MiRs are small, non-coding regulatory RNAs, which are typically 18–24 nucleotides long. In human, miRs have been associated with cardiovascular disease by targeting the abundant of protein-coding genes that modulate cell growth, proliferation, apoptosis, and

hypertrophy (Gupta, et al., 2016, Barwari, et al., 2016). Most of miRs can be detected not only within different types of cells, but also in different biological fluids and cell culture media *in vitro*, which are commonly called circulating miRs or extracellular miRs (Hunter, et al., 2008). The reason why circulating miRs are detectable lies in their remarkable stability and resistance to degradation by endogenous RNase (Tsui, et al., 2002). Circulating miRs are either encapsulated by different types of EVs or bound to proteins that prevent them from being digested (Arroyo, et al., 2011, Turchinovich, et al., 2011). The releasing of miRs is altered under different physiological and pathological conditions (Jansen, et al., 2016). Acute myocardial infarction patients have a significantly higher level of several miRs in their plasma compared to control subjects. In contrast, a reduction in the level of some circulating miRs have also been reported in heart failure patients (Zhang, et al., 2016, Ovchinnikova, et al., 2016). Therefore, circulating miRs have been investigated widely as biomarkers in many cardiovascular diseases.

In clinical practice, the assessment of several hemodynamic parameters such as velocity, gradients, and aortic valve area, helps with the classification and effective treatment of AS by TAVR (Nishimura, et al., 2018). However, even in patients who meet the criteria for TAVR, some of them still do not obtain hemodynamic improvement or clinical benefit (Herrmann, et al., 2014). In AS patients with reduced LVEF, some of them developed improved LVEF after afterload reduction while some don't. Previous studies have shown that circulating miRs are differentially regulated in various conditions. For instance, miR-423-5p was highly expressed in heart failure patients compared with healthy controls and circulating microRNA-30d is associated with the response to cardiac resynchronization therapy in heart failure (Melman YF, et al., 2015, Tijsen, et al., 2010). Although miRs and EVs have been widely studied in cardiovascular diseases, however, their roles are still not clear in AS patients after TAVR.

1.4 Aims

Therefore, the specific aims of this study can be outlined as follows:

1. To explore whether circulating miRs are differently regulated as a response to TAVR in reduced LVEF patients.
2. To explore the biological function of miRs mediated by EVs in cardiovascular cells.

2. Materials and Methods

2.1 Materials

Tab. 1: Information of key resources

Materials	Company	Catalog number
Chemicals and reagents		
DAPI	Vector laboratories	H-1200
Hsa-miR-122-5p inhibitor	Thermo Fisher Scientific	4464084
Hsa-miR-122-5p mimic	Thermo Fisher Scientific	4464066
Hydrogen peroxide solution	SIGMA-Aldrich	H1009
Lipofectamine RNAiMAX	Thermo Fisher Scientific	13778150
PKH67	SIGMA-Aldrich	MIDI67
Proteinase K	Thermo Fisher Scientific	25530049
RNase A	Thermo Fisher Scientific	AM2271
RiboLINK miRNA red	Riboxx	L-00212
TaqMan Array Human Apoptosis	Thermo Fisher Scientific	4414072
TaqMan Array Human MicroRNA A+B Cards	Thermo Fisher Scientific	4444913
Triton X-100	Sigma-Aldrich	9002-93-1
TRIzol	Thermo Fisher Scientific	15596018
Commercial Kits		
FITC Annexin V Apoptosis Detection Kit with 7-AAD	BioLegend	640922
LDH Cytotoxicity assay kit	Thermofisher	88953
MTT Cell Growth Assay Kit	Millipore	CT02
TaqMan microRNA reverse transcription kit	Thermo Fisher Scientific	4366596
Cells and medium		
Human Coronary Artery Endothelial Cells (HCAEC)	Promocell	C-12221
Human Cardiac Myocytes (HCM)	Promocell	C-12810

Materials	Company	Catalog number
Endothelial Cell Growth Medium MV	promocell	C-22020
Myocyte Growth Medium	promocell	C-22070
Primers		
BIRC8	Thermo Fisher Scientific	Hs01057786
BCL2	Thermo Fisher Scientific	4331182
Caenorhabditis elegans miR-39	Thermo Fisher Scientific	478293
Hsa-miR-122	Thermo Fisher Scientific	002245
Hsa-miR-1274a	Thermo Fisher Scientific	002883
Hsa-miR-133a	Thermo Fisher Scientific	002246
Hsa-miR-192	Thermo Fisher Scientific	002272
Hsa-miR-223	Thermo Fisher Scientific	002098
Hsa-miR-26a	Thermo Fisher Scientific	000405
Hsa-miR-483-5p	Thermo Fisher Scientific	002338
Hsa-miR-720	Thermo Fisher Scientific	002895
Hsa-miR-885-5p	Thermo Fisher Scientific	002296
Hsa-miR-let-7b	Thermo Fisher Scientific	002619
NAIP	Thermo Fisher Scientific	Hs03037952
NOD2	Thermo Fisher Scientific	Hs01550753
Antibodies		
Anti-beta-Actin antibody	Sigma-Aldrich	A1978
Anti BCL2 Rabbit Polyclonal	Proteintech	12789-1-AP
Anti-Mouse IgG	Sigma-Aldrich	A9044-2ML
Anti-Rabbit IgG	Sigma-Aldrich	A9169-2ML
Equipment		
Applied Biosystems 7500HT Real-Time PCR	Thermo Fisher Scientific	-
Applied Biosystems 7900HT Real-Time PCR	Thermo Fisher Scientific	-
Falcon Permeable Support for 12-well Plate with 1.0 μm	Corning	353103
Optima LE-80K Ultracentrifuge	Beckman Coulter	-

2.2 Methods

2.2.1 Study subjects

931 patients presenting in the outpatient and emergency departments of the University Hospital Bonn were enrolled in our study between 2008 and 2016. All clinical samples and measurements were obtained with informed consent from the patients. First, six of them were matched and used as a screening cohort for the miR array. The exclusion criteria included: (i) LVEF>45 % at baseline; (ii) severe aortic regurgitation; (iii) lost to follow-up; (iv) malignant, inflammatory disease or severe renal dysfunction; (v) incomplete blood sample. They were divided into two groups based on LVEF improvement (n=3, respectively) at six months after TAVR: robust improvement (>15 %) and no improvement (≤0 %). Next, from the 925 patients that were left, we further excluded 835 patients based on exclusion criteria. Therefore, 90 patients were selected as validation cohort and were classified into three groups: robust improvement (>15 %, n=34), mild improvement (0-15 %, n=37), and no improvement (≤0 %, n=19). They were selected to quantify the expression of miRs based on the miR array results. Among these patients from the screening and validation cohorts, plasma samples were collected and measured at day -1 (the day before TAVR), day 1 (the day after TAVR), and day 7.

2.2.2 Blood sample preparation

Blood samples were collected under sterile conditions from the cubital vein and buffered by using sodium citrate or ethylenediaminetetraacetic acid (EDTA). To generate platelet-derived plasma samples, the blood was first centrifuged at 1500 × g for 15 minutes followed by centrifugation at 13,000 × g for two minutes to generate platelet-deficient plasma. Samples were then stored at −80 °C until the miR levels were analyzed. Repeated freeze-and-thaw cycles were avoided.

2.2.3 Taqman miR array

Total RNA (500 ng) from the plasma of patients with robust LVEF improvement (n=3) and no LVEF improvement (n=3) were converted to cDNA by priming with a mixture of looped primers (Human MegaPlex Primer Pools, Applied Biosystems). Samples were assessed using TaqMan® Array miR Cards (Applied Biosystems) for a total of 384 unique assays specific to human miRs under standard real-time PCR conditions. The PCR was carried out on an Applied Biosystems 7900 HT Real-Time PCR System. Data analysis was performed using the Data Analysis v3.0 Software (Applied Biosystems). CT values above 37 were defined as undetectable.

2.2.4 RNA isolation and qRT-PCR

Total RNA was extracted and isolated by using the TRIzol method, according to the manufacturer's instructions. Caenorhabditis elegans miR-39 (cel-miR-39, 5 nM, Qiagen) was spiked in for normalization when isolating RNA from plasma. The total RNA concentration was quantified by using a Nanodrop spectrophotometer (Nanodrop Technologies). Then total RNA was reverse transcribed, according to the manufacturer's protocol. MiRs or mRNAs were detected by using TaqMan® miR/gene expression assays (Applied Biosystems) on a 7500 HT Real-Time PCR machine (Applied Biosystems). For all miRs/mRNAs, a CT value above 45 was defined as undetectable. Values are expressed as $2^{-[CT(miR)-CT(control)]}$ $\log_{10}$ and samples were run in triplicate.

2.2.5 Cell culture and generation, centrifugation of extracellular vesicles

Human coronary artery endothelial cells (HCAECs) and cardiac myocytes (CMs) (PromoCell) were cultured in cell growth basal media with growth media supplement mix (PromoCell, # C-22020, C-22070) under standard conditions (37 °C, 5% CO2). Cells from passages 6–8 were used when they were 70–80% confluent. After treatment based on various experimental designs, confluent cells were starved by incubating them in a basal medium (without growth media supplements) for 24 hours and the supernatant was collected for centrifugation after starvation. To isolate MVs from the supernatant of the

culture medium or plasma, samples were first centrifuged at 2000 × g, 4 °C for 15 minutes to remove cellular debris. The supernatant was collected and centrifuged again at 20,000 × g, 4 °C for 40 minutes to pellet the MVs. The MV pellet was resuspended in sterile ice-cold PBS followed by re-centrifugation (20,000 x g, 4 °C, 40 minutes) to purify the MVs. The pure MV pellet was resuspended in sterile 1 x PBS and used freshly. To pellet the exosomes, the supernatant without MVs was collected again and centrifuged at 100,000 × g, 4 °C for 90 minutes in a Beckman Coulter OptimaTM LE-80K Ultracentrifuge with a Type SW 41Ti rotor (k-factor: 256.6). The pellet was resuspended in sterile ice-cold PBS followed by re-centrifugation at 100,000 × g, 4 °C for another 90 minutes to purify the pellets. Finally, the purified pellet was resuspended in sterile 1 x PBS and used immediately.

2.2.6 Oxidative stress stimulation on endothelial cells

To generate oxidative-stress-stimulated MVs from ECs, confluent HCAECs were treated with PBS as a control, 150 µm H_2O_2, or 300 µm H_2O_2 (SIGMA-Aldrich, H1009) for 24 hours. They were then subjected to basal media without growth supplements for 24 hours to generate different oxidative-stress-stimulated MVs for further RNA isolation and analysis.

2.2.7 Transfection of endothelial cells and cadiac myocytes

Cells at 50–70 % confluence were transfected with 20 nM miR-122-5p mimic (Thermo Fisher Scientific, MC11012), inhibitor (Thermo Fisher Scientific, MH11012), miR negative control (Thermo Fisher Scientific, 4464078) for ECs and 50 nM mimic, 70 nM inhibitor, 50 nM miR negative control for CMs, using Lipofectamine RNAiMAX (Thermo Fisher Scientific) for 24–72 hours, according to the manufacturer’s protocol.

2.2.8 Microvesicle RNA degradation assay

MVs were resuspended in PBS. The sample from the untreated group was left on ice as a normal control. To digest the protein, 45 µl Proteinase K (Thermo Fisher Scientific, #25530049) were added to the next sample. Additionally, 25 µl Triton X-100 (Sigma-

Aldrich, #T8787) were added to another sample for 30 minutes at 37°C to disrupt the membrane bilayer of the MVs. Afterwards, all samples were treated with 5 µl RNase A (Thermo Fisher Scientific, #AM2271) for 10 minutes at 37°C. Finally, the samples were lysed with Qiazol, and RNA was isolated for qRT-PCR analysis (normalized to spiked-in cel-miR-39).

2.2.9 Intercellular transfer of MVs into recipient cells by flourescent microsopy

ECs were transfected with 20 nM cyanine 3 (Cy3)-labeled miR-122-5p (Riboxx, #L-00212) for 24 hours. On the day after transfection, ECs were washed three times and serum-free culture medium was added for 24 hours to generate MVs. MVs were then isolated and stained with PKH67 (SIGMA-Aldrich, #MIDI67), a green fluorescent cell-labeling dye, according to the manufacturer's instructions. PKH67-labeled MVs were washed twice with PBS. Recipient cells were co-incubated with the labeled MVs for 24 hours. Finally, the nuclei were stained with DAPI (Vector laboratories, #H-1200). Zeiss Axiovert 200M microscope and ZEN 2.3 pro software were used to visualize the uptake of MVs into the recipient cells.

2.2.10 Apoptosis assay

150 µm H_2O_2 was added to 6-well plates to induce apoptosis in the cells for 24 hours. Cells were then dissociated from the surface and washed twice with cold BioLegend's Cell Staining Buffer then resuspended in Annexin V Binding Buffer. 5 ml FITC Annexin V and 7-AAD Viability Staining Solution were added to 100 µl cell suspension in a 5 ml test tube and incubated for 15 minutes at room temperature in the dark. 400 µl of Annexin V Binding Buffer was added to each tube. Cells were analyzed by FACSCalibur (BD Biosciences). Apoptotic cells were defined as those that were FITC-positive.

2.2.11 MTT assay

Pre-transfected cells were transferred into a 96-well plate at 8000 cells/well. Next, 100 µM H_2O_2 was added and the cells were incubated at 37°C and 5% CO_2 for 24 hours. 0.01 ml

AB Solution from an MTT Cell Growth Assay Kit (Sigma-Aldrich, #CT02) was added to each well and incubated at 37°C for 4 hours. 0.1 ml isopropanol with 0.04 N HCl was added to each well and mixed thoroughly with a multichannel pipette. The absorbance was measured on an ELISA plate reader with a test wavelength of 570 nm and a reference wavelength of 630 nm.

2.2.12 Cytotoxicity assay

Total lactate dehydrogenase (LDH) activity in cell lysates was examined using the LDH cytotoxicity assay kit (Thermofisher, #88953.) according to the manufacturer's instructions. Briefly, cells were seeded in a 96-well plate and treated with 100µM H_2O_2 one day prior to the assay to induce cytotoxicity and subsequent release of LDH. Medium was transferred to a new plate the next day and mixed with reaction mixture. After 30 minutes of incubation at room temperature, the reactions were stopped by adding a "stop" solution. Absorbance at 490 nm and 680 nm was measured using an ELISA plate reader (TECAN, Infinite M200 Microplate reader) to determine the LDH activity.

2.2.13 TaqMan Gene Expression PCR array

Total RNA was extracted from CMs and the RNA was quantified by using a Nanodrop instrument. Reverse transcription was performed using a Reverse Transcription Kit. Then a Taqman human apoptosis array that includes 93 apoptosis-related genes and 3 housekeeping control genes (18S, ACTB, GAPDH) was performed by using a 7500 HT real-time PCR machine (Applied Biosystems). The comparative cycle of threshold (Ct) method was performed to calculate the relative expression of the transcripts.

2.2.14 Western Blot

Cells were homogenized with RIPA buffer (150 mM NaCl, 1.0 % Nonidet P-40, 0.5 % deoxycholate, 0.1 % SDS, and 50 mM Tris, pH 8.0) containing 1 mM Na_3VO_4, 5mM NaF and protease inhibitor cocktail (Roche) at 4°C. Protein concentration was measured using Lowry protein assay (BioRad, #500-0116). Equal amounts of proteins (30 µg) were loaded

onto 4–15% Precast Protein Gels for electrophoresis (BioRad, #4561084), transferred onto a PVDF membrane, and blocked with 5 % BSA for 1 hour. The blots were incubated with anti-Bcl2 (Proteintech 12789-1-AP). Detection was performed by using the appropriate secondary antibody (Anti-Rabbit IgG, Abcam) and proteins were revealed by chemiluminescence using the ECL kit (GE healthcare, #RPN2232). Beta-actin (Sigma-Aldrich, A1978) was used as the loading control.

2.2.15 Statistical analysis

Normally distributed continuous variables were presented as the mean ± SD. Continuous variables were tested for a normal distribution with the use of the Kolmogorov–Smirnov test. Categorical variables were presented as frequencies and percentages. For continuous variables, Student t-test or Mann–Whitney U was used for comparison between two groups. For the comparison of >2 groups, the epeated measures ANOVA with Bonferroni's correction for multiple comparisons test was used. For the comparison of miR expression in plasma at three different time points, the 2-way ANOVA with Tukey's correction for multiple comparisons test was used. A Chi-square test was used for the categorical data. All tests were 2-sided and statistical significance was assumed when the null hypothesis could be rejected at $p < 0.05$. Statistical analysis was performed with IBM SPSS Statistics version 24 (USA) and GraphPad Prism 8.

3. Results

3.1 Identification of target miRs as biomarker for heart function after TAVR

As miRs are known as biomarkers and effectors of heart function, the main aim of this study was to explore whether circulating miRs are differently regulated after TAVR in reduced LVEF patients. We therefore analysed the level of circulating miRs in these patients. An overview of the clinical design for the miRs study in TAVR patients is shown in Figure 2. Between January 2008 and July 2016, 931 patients with severe symptomatic aortic stenosis receiving TAVR at the Heart Center Bonn were enrolled in the study. Based on the degree of LVEF improvement at six months after TAVR, we first entrolled six patients as the screening cohort for the miR array. They were matched and selected based on the exclusion criteria and were divided into two groups: robust improvement (>15%) or no improvement (≤0%) (n=3, each). There was no difference in the baseline characteristics of the patients in the screening cohort (Table 2). Plasma samples from each patient were collected at three different time points: the day before the procedure (pre-TAVR, day -1), day 1, and day 7 after the procedure. To identify the alteration of expression of circulating miRs in different groups, we performed a PCR-based human miR array of the samlpes from two groups of patients at these three time-point. The microRNA levels of each patient at each time-point were measured and calculated. We then compared the microRNA level between diffrernt time-point in different groups. Eight miRs were shown to be differently regulated. In the no-improvement group, levels of miR-26a, miR-122, miR-192, miR-483-5p, miR-720, miR-885-5p, miR-1274a were elevated at day 7 when compared with day 1, while in robust-improvement group, level of miR-233 was increased at day 1 when compared with day -1 (Figure 3, 4). Based on the literature, we also quantitated four miRs that are related to LV function and fibrosis (miR-21, miR-145, miR-199, and miR-30b). Therefore,12 miRs were selected for further prospective quantification.

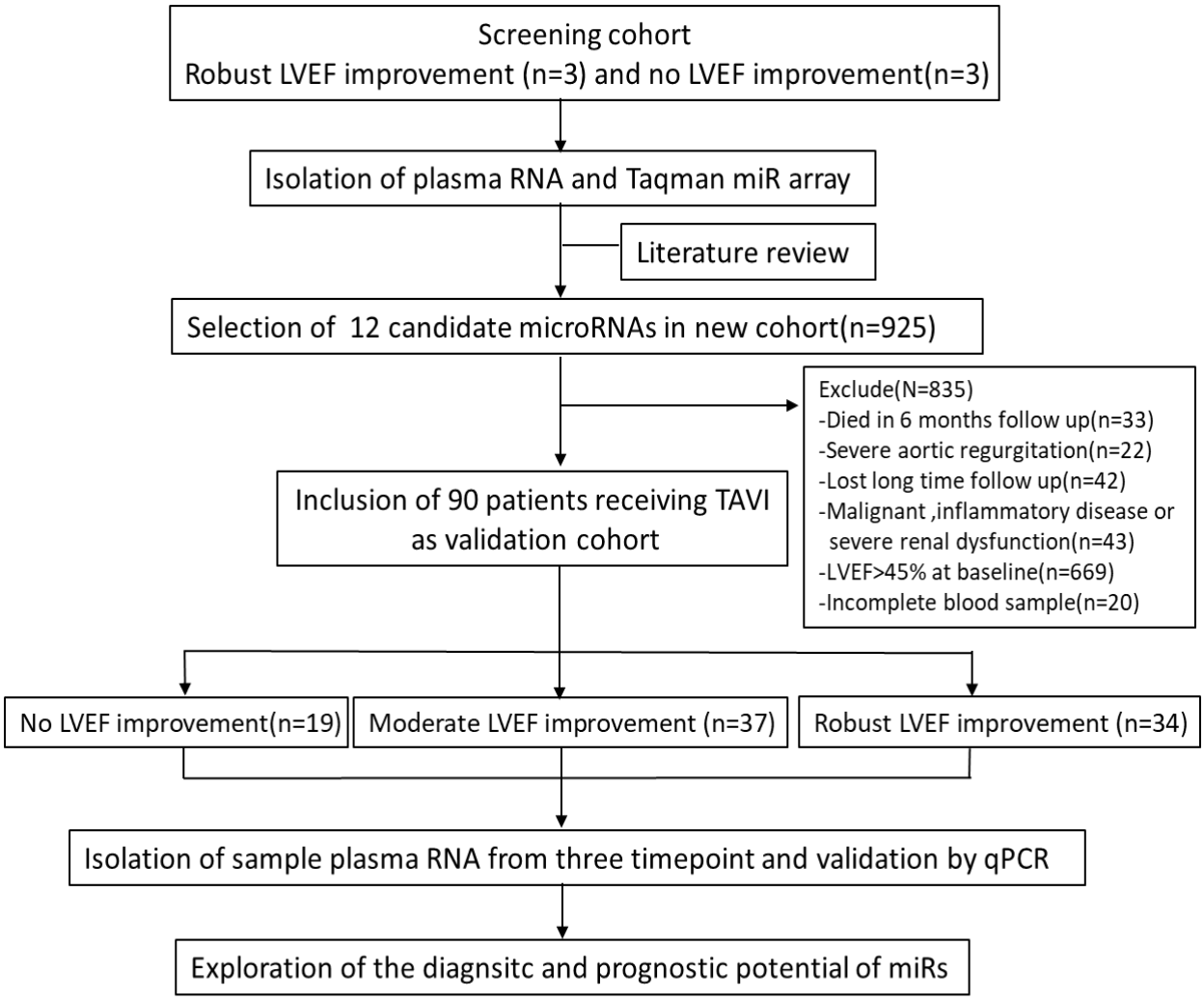

Fig. 2: Study flow for identifying circulating miRs. According to the protocol, we performed a miR array to screen for candidate miRs in the plasma of patients. To validate the microarray results, 90 patients who fulfilled the criteria were divided into three groups depending on LVEF improvement at 6 months after TAVR based on echocardiography data. Robust improvement (>15%), moderate improvement (0-15%), and no improvement (≤0%).

Sample group	No improvement group							Robust improvement group
Time point	Day7 vs. Day1							Day1 vs. Day-1
MiR ID	26a	885-5p	483-5p	1274a	192	720	122	223
FC	2.86	3.89	4.03	4.12	4.32	6.60	10.29	3.14
P	0.024	0.014	0.028	0.012	0.023	0.049	0.006	0.022

Fig. 3: Summary of all the differentially regulated miRs in miR screening. Samples from day-1, day1, day7 of each patient were tested. Six patients from robust improvement (>15%) and no improvement (⩽0%) (n=3, each) were selected for miR screening. The screening was performed using TaqMan miR array. Data were compared by different time points in different groups as presented.

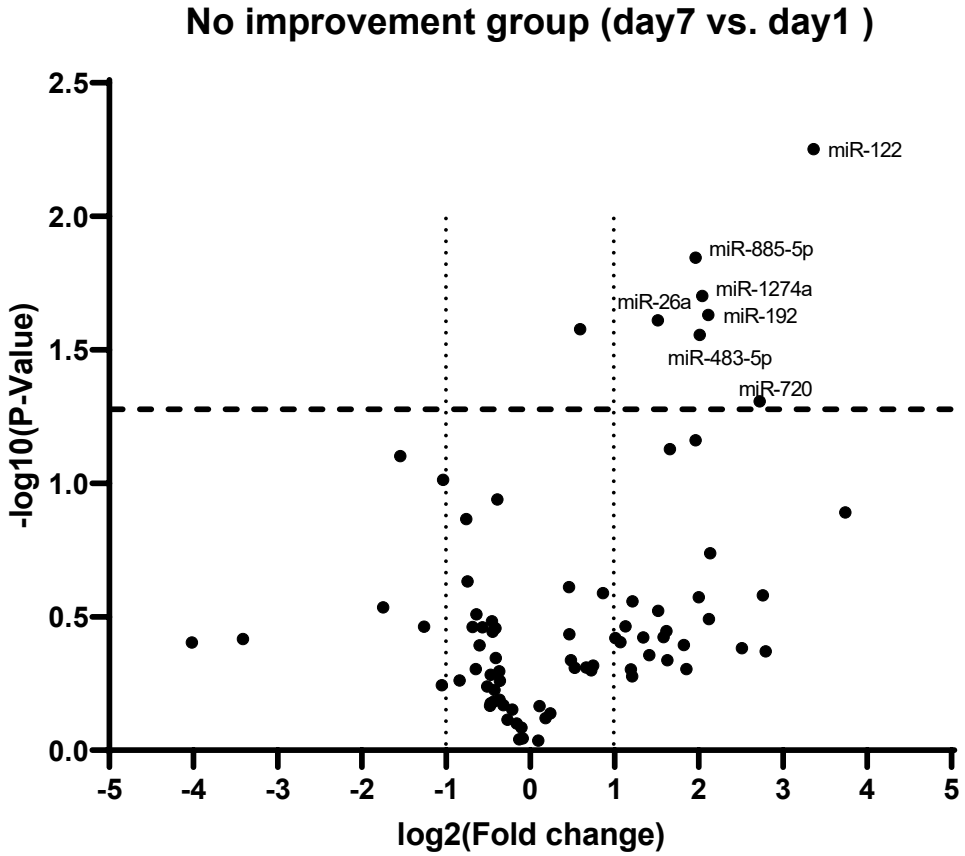

Fig. 4: Representative volcano plot of the differentially regulated miRs in no improvement group. Upregulated miRs are shown in the plot (miRs with Fold change>2 and P<0.05 were labelled). In the no-improvement group, samples from day 7 were compared with day 1. Thresholds of a greater than two-fold difference (gray vertical lines) and a p-value <0.05 (horizontal line) were applied.

Tab. 2: Baseline characteristics of the discovery cohort

	No LVEF improvement (≤0 %)	Robust LVEF improvement (>15 %)	p-value
Total population	3	3	-
Age	82.3±6.0	80.7±8.2	0.79
gender (Male)	1(33.33 %)	1(33.33 %)	-
NYHA class	3.33±0.58	2.67±0.58	0.23
Body mass index	25.8±1.4	30.4±9.8	0.47
Diabetes Mellitus	1(33.3%)	0(0 %)	1
Coronary artery disease	1(33.3 %)	1(33.3 %)	-
Chronic obstructive pulmonary disease	1(33.3 %)	0(0 %)	1
Atrial fibrillation	3(100%)	1(33.3%)	0.40
Previous myocardial infarction	1(33.3 %)	0(0 %)	1
eGFR	36.0±4.2	57.4±7.4	0.11
Euro score II	7.0±2.9	19.9±14.4	0.34
STS	11.7±13.0	5.2±1.6	0.61
Baseline LVEF	37.3±7.5	33.3±7.6	0.55
LVEF at 6 months	31.3±8.1	50.3±6.7	0.04

NYHA, New York heart association; eGFR, estimated glomerular filtration rate; Euro score II, the european system for cardiac operative risk evaluation II; STS, thoracic surgeons score; LVEF, left ventricular ejection fraction.

3.2 Validation of plasma miR biomarkers for LVEF improvement after TAVR

We next validated the findings in our validation cohort. From the screening cohort, we found eight miRs that were shown to be differently regulated. We also included four miRs that are related to LV function and fibrosis. We therefore validated these twelve miRs as candidate target in the validation cohort. To confirm the validation cohort, we further excluded 835 patients from 925 patients based on exclusion criteria. The exclusion criteria include: (i) LVEF >45 % at baseline, n=669; (ii) severe aortic regurgitation, n=22; (iii) lost to follow-up, n=75; (iv) malignant, inflammatory disease or severe renal dysfunction, n=43; (v) incomplete blood sample, n=20. Therefore, 90 patients were selected for further validation. They were divided into three groups based on the degree of LVEF improvement at six months after TAVR: robust improvement (>15%, n=34), moderate improvement (0-15%, n=37) or no improvement ($\leqslant$ 0%, n=19). The baseline characteristics for the validation cohort are presented in Table 3. There was no significant difference with respect to age or gender among the three groups. Comorbidities that could influence prognosis of TAVR patients, such as pulmonary disease and CAD, were similar between the groups. Of note, patients with no LVEF improvement had an increased level of troponin, while those from robust-improvement groups had a decrease in troponin at six months. Plasma samples from each patient were collected at three different time points: the day before the procedure (day -1), day 1, and day 7 after the procedure. To identify the expression of circulating miRs, we isolated the miRs from the plasma samples, performed the qRT-PCR and compared the miR level of different groups at different time-points.

Tab. 3: Baseline characteristics of the validation cohort

	Total	No improvement	Moderate Improvement	Robust Improvement	p-value
Total population	90	19	37	34	-
Age	80.0±6.2	81.7±76.3	79.1±6.2	79.9±6.1	0.35
Male gender	68.9	12(63.2 %)	78.4	61.8	0.27
NYHA level	3.2±0.5	3.3±0.5	3.1±0.5	3.2±0.5	0.45
Body mass index	25.1±5.4	25.2±3.7	24.3±6.7	25.8±4.9	0.56
Diabetes Mellitus	21 (23.3 %)	7 (36.8 %)	7 (18.9 %)	7 (20.6 %)	0.30
Coronary artery disease	59 (65.66 %)	13 (68.4 %)	24 (64.9 %)	22 (64.7 %)	0.96
COPD	25 (27.8 %)	6 (31.6 %)	8 (21.6 %)	11 (32.4 %)	0.56
Atrial fibrillation	47 (52.2 %)	12 (53.2 %)	19 (51.4 %)	16 (47.1 %)	0.54
Previous myocardial infarction	14 (15.6 %)	5 (16.3 %)	5 (13.5 %)	4 (11.8 %)	0.35
Euro score II	10.5±7.7	9.8±7.4	10.1±8.7	12.0±8.4	0.48
STS score	8.0±5.9	8.3±5.8	6.7±4.7	9.0±6.9	0.11
eGFR	53.6±18.3	54.2±15.8	51.6±20.0	53.0±15.6	0.96
Mild-Severe mitral regurgitation	51 (56.7 %)	11 (57.9 %)	24 (64.9 %)	16 (47.1 %)	0.32
Laboratory parameters					
CKMB day -1	2.2±1.6	2.6±2.5	2.2±1.3	2.1±1.1	0.56
CKMB day 7	1.7±1.1	1.7±1.3	1.7±1.0	1.7±1.2	0.97
CKMB 6 months	2.2±1.7	2.3±1.7	2.1±1.7	2.2±1.9	0.90
CKMB change (6 month – day -1)	-0.03±1.38	-0.16±0.73	0.13±1.31	-0.14±1.70	0.66
Troponin day -1	0.07±0.10	0.03±0.02	0.08±0.13	0.08±0.10	0.22
Troponin day 7	0.16±0.33	0.25±0.56	0.15±0.30	0.13±0.13	0.44
Troponin 6 months	0.05±0.12	0.09±0.09	0.06±0.06	0.02±0.02	0.11
Troponin change (6 months – day -1)	0.02±0.14	0.06±0.16	-0.02±0.14	-0.05±0.10	0.01
Baseline echocardiography					
LVEF day -1	35.3±7.5	38.5±4.1	35.5±6.6	33.4±9.3	0.18
LVEF day 7	42.8±12.1	35.6±7.0	40.9±9.7	49. 0±14.0	0.00
LVEF 6 months	45.7±11.0	34.6±5.1	43.6±7.4	54.3±10.2	0.00
LVEF change (6 months – day -1)	10.4±10.4	-3.9±3.6	8.1±4.6	20.9±5.2	0.00
LVEDVi day -1	80.1±31.3	81.7±30.1	82.3±34.4	76.9±29.9	0.79

	Total	No improvement	Moderate Improvement	Robust Improvement	p-value
LVEDVi day 7	77.1±31.4	87.5±37.0	77.3±34.8	71.3±24.1	0.24
LVEDVi 6 months	65.6±27.2	78.9±35.4	64.8±26.1	58.2±19.1	0.03
LVEDVi change (6 months – day -1)	12.70±25.8	-2.8±23.7	-18.4±26.1	-13.7±26.0	0.13
SVI day -1	29.1±11.6	32.0±11.1	28.7±10.7	27.8±12.7	0.46
SVI day 7	32.2±14.5	32.7±17.8	28.5±11.9	34.7±14.3	0.31
SVI 6 months	28.4±9.4	25.7±9.0	26.8±10.7	31.4±7.5	0.31
SVi change (6 months – day -1)	-0.8±11.6	-5.7±-2.3	-2.3±9.7	3.5±12.2	0.02
IVSd day -1	1.19±0.23	1.21±0.23	1.23±0.24	1.1±0.22	0.24
IVSd 6 month	1.16±0.23	1.12±0.19	1.18±0.19	1.16±0.29	0.68
PWd day -1	1.16±0.24	1.16±0.21	1.15±0.22	1.17±0.29	0.93
PWd 6 month	1.19±0.24	1.1±0.19	1.21±0.22	1.22±0.29	0.39
Transvalvular gradient >40 mmHg	30 (38.0 %)	4 (21.1 %)	9 (31.0 %)	17 (54.8 %)	0.04

Baseline demographic, laboratory and echocardiographic parameters of the validation study population. p-values reflect the comparison between three different groups. CKMB, Creatine kinase-MB; LVEDVi, LV end-diastolic volume index; SVI, Stroke Volume Index; IVSd, interventricular septal diameter; PWd, posterior wall diameter.

When we studied miR expression in the validation cohort, it showed that miR-122 level was significantly lower in mild- or robust- improvement groups compared with no-improvement group at day 7 after TAVR (Figure 5). Interestingly, as the LVEF became worse in no-improvement group, the miR-122 level increased at day 7 after TAVR when compared to its baseline level at day -1. MiR-1274a also showed similar trend, with increasing expression in moderate-improvement group (p=0.0014), but there is no significant difference in no-improvement group (p=0.15). As miR-199 showed poor expression (low sample number with qualified expression) and miR-21 gave an unspecific trend, we didn't enroll them for further analysis although they had significant p-values.

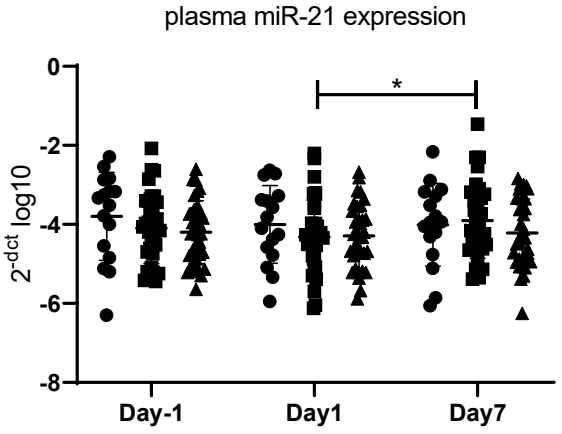
plasma miR-21 expression
0
-2
-4
-6
-8
2-dct log10
*
Day-1
Day1
Day7

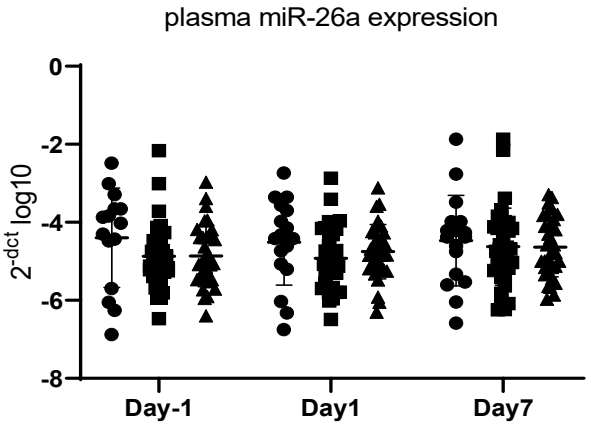
plasma miR-26a expression
0
-2
-4
-6
-8
2-dct log10
Day-1
Day1
Day7

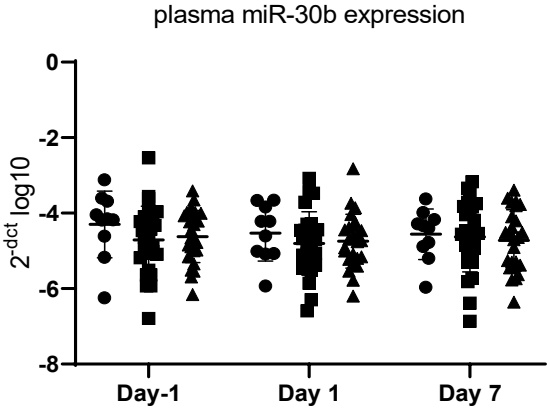
plasma miR-30b expression
0
-2
-4
-6
-8
2-dct log10
Day-1
Day 1
Day 7

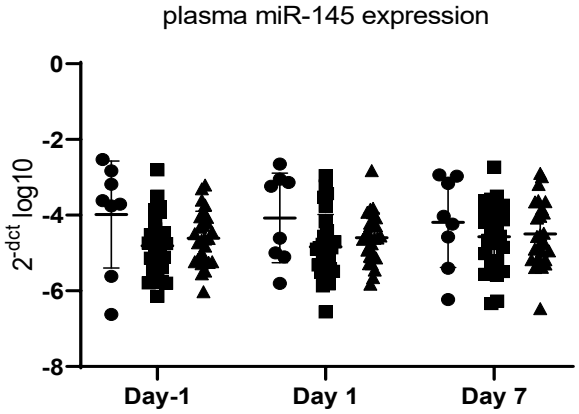
plasma miR-145 expression
0
-2
-4
-6
-8
2-dct log10
Day-1
Day 1
Day 7

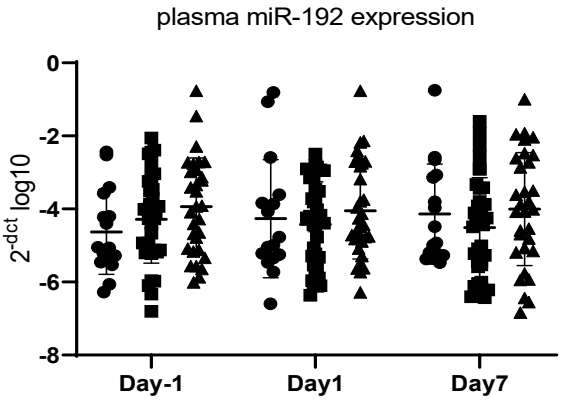
plasma miR-192 expression
0
-2
-4
-6
-8
2-dct log10
Day-1
Day1
Day7

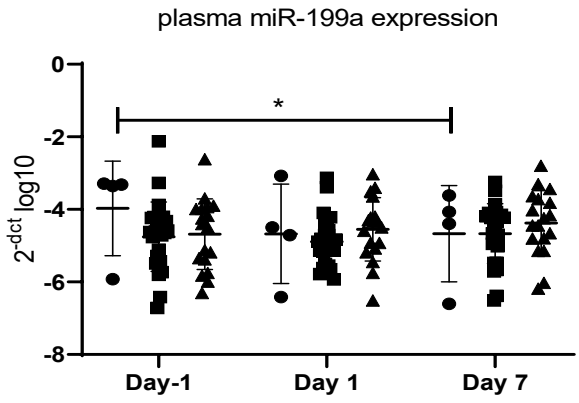
plasma miR-199a expression
0
-2
-4
-6
-8
2-dct log10
*
Day-1
Day 1
Day 7

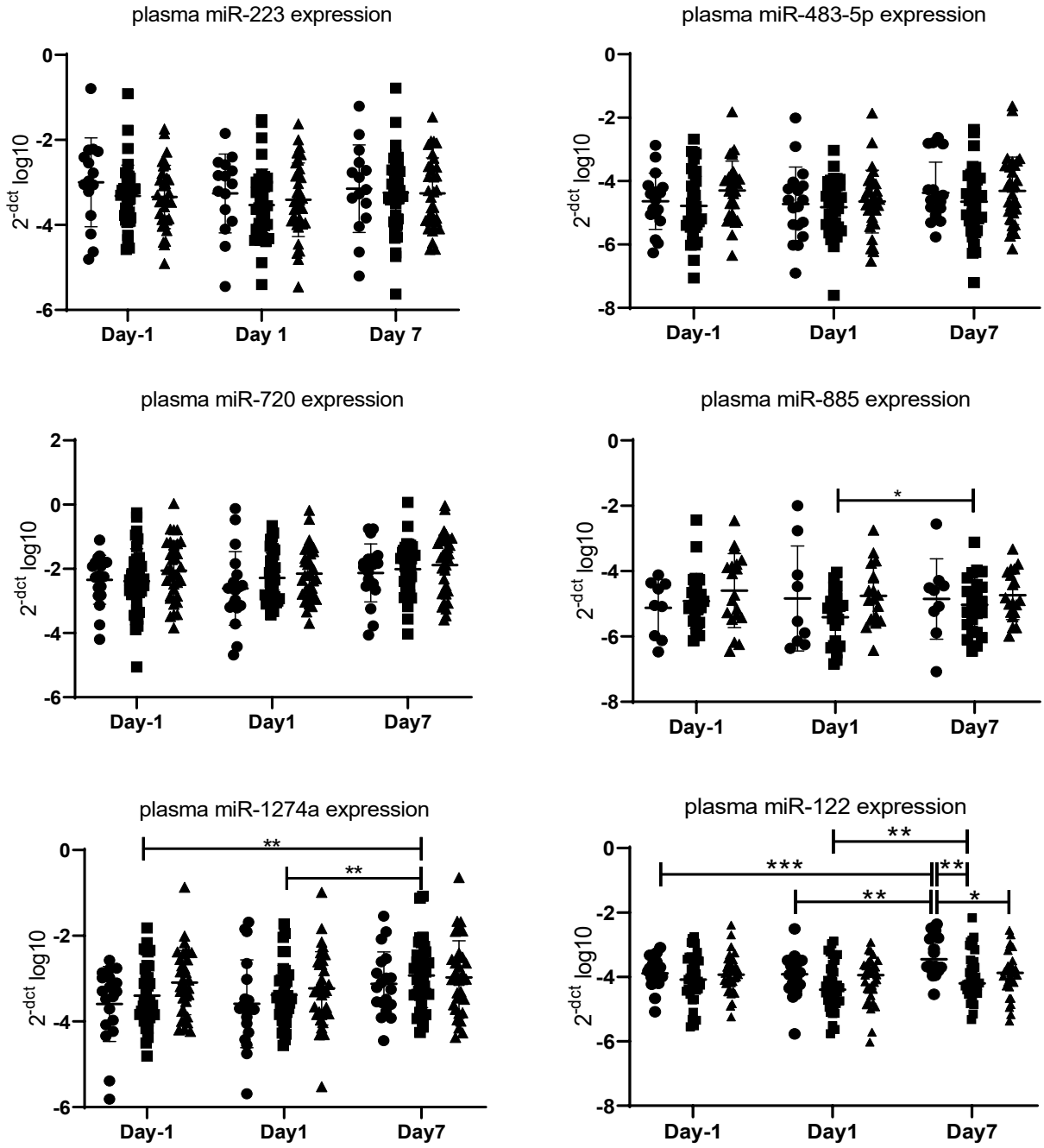

Fig. 5: MiR expression in low LVEF patients undergoing a TAVR procedure. Circulating miR expression was analyzed in 90 patients at three different time points (day -1, day 1, day 7). Values were normalized to cel-miR-39 and were expressed as $2^{-[CT(miR)-CT(cel\text{-}miR\text{-}39)]}$ $\log_{10}$. Data are represented as mean±SD (*p<0.05, **p<0.01, ***p<0.001) by repeated meausres ANOVA with Tukey's multiple comparisons test.

As the other miRs examined for validation failed to show significant differences and miR-122 is associated with LVEF improvement, we decided to explore the role of miR-122 in LVEF improvement after TAVR based on these observations. An increase in the level of miR-122 at day 7 was negatively correlated with improvement of LVEF at day 7 and also at six months after TAVR (r=-0.264, -0.328, respectively; $p<0.05$; Figure 6A, 6B). Additionally, we also observed that in patients with relatively higher LVEF at baseline (>45 %), the miR-122 level was lower than in patients with reduced LVEF, which suggested the miR-122 level is associated with LVEF (Figure 6C). In a ROC analysis, the increase of miR-122 was a significant discriminator for adverse LVEF recovery (statistic 0.757, 95 % CI =0.651-0.863, P=0.006) (Figure 7A, left). Next, we grouped the patients by the median of ΔmiR-122 level (day 7 – day -1) and made a Kaplan–Meier cumulative survival analysis. The result showed that in a three-year follow-up, patients with a high ΔmiR-122 level (miR-122 level significantly increased at day7 after TAVR) displayed a reduced MACE-free survival rate (p=0.03) than low ΔmiR-122 patients (miR-122 decreased at day7) (Figure 7A, right). As we noticed an increase in the average troponin level at 6 months after TAVR in no-LVEF improvement group (Table 3), we then compared the alteration of troponin level in patients with a different response after TAVR. We found that a significantly higher percentage of patients in the no-improvement group had an increased troponin level compared to moderate- and robust-improvement group (p=0.004) (Figure 7B, left). Furthermore, when grouped the patients by the alteration of miR-122 (increased at day7 vs. decreased at day7), we found that the group with increased miR-122 also had an increased troponin level at 6 months after TAVR (p=0.014), indicating the positive correlation between the miR-122 level and troponin level, a known biomarker for cardiac injury (Figure 7B, right).

A

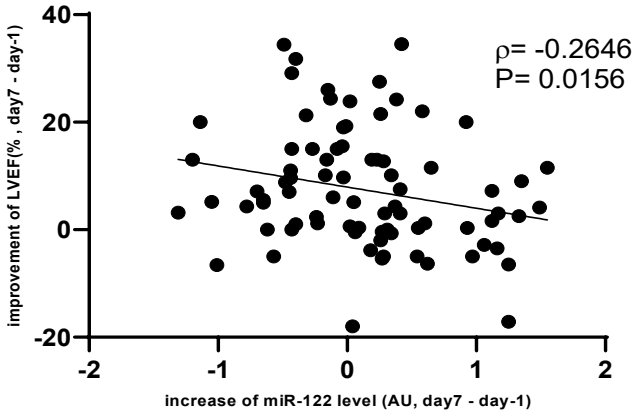

B

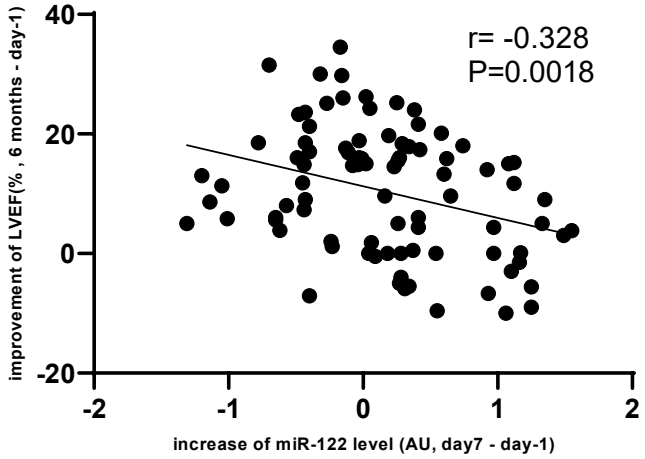

C

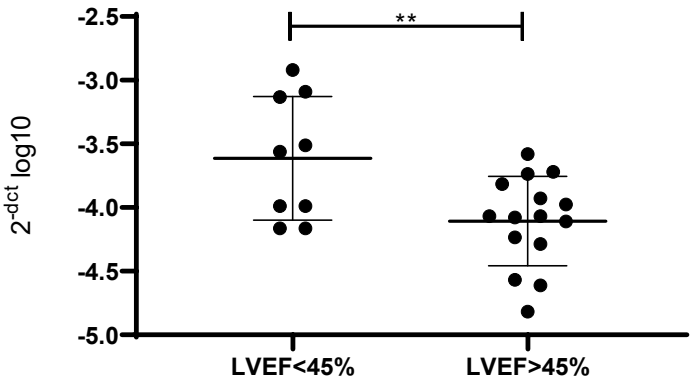

Fig. 6: MiR-122 is associated with LVEF improvement after TAVR. (A) Correlation between change of miR-122 and LVEF level at day 7. Association is significant with Spearman coefficient of -0.265, p=0.015. (B) Correlation between change of miR-122 and LVEF level at 6 months (Pearson coefficient of -0.328, p=0.002). (C) Differential expression of miR-122 level in patients with higher or lower LVEF. Samples at baseline (day -1) from patients with relatively low LVEF (<45 %; n=9) and higher LVEF (>45 %; n=15) were analyzed. Values were normalized to cel-miR-39 and were expressed as 2-[CT (miR)-CT(cel-miR-39)] log10. Data are presented as the mean ± SD(**p<0.01).

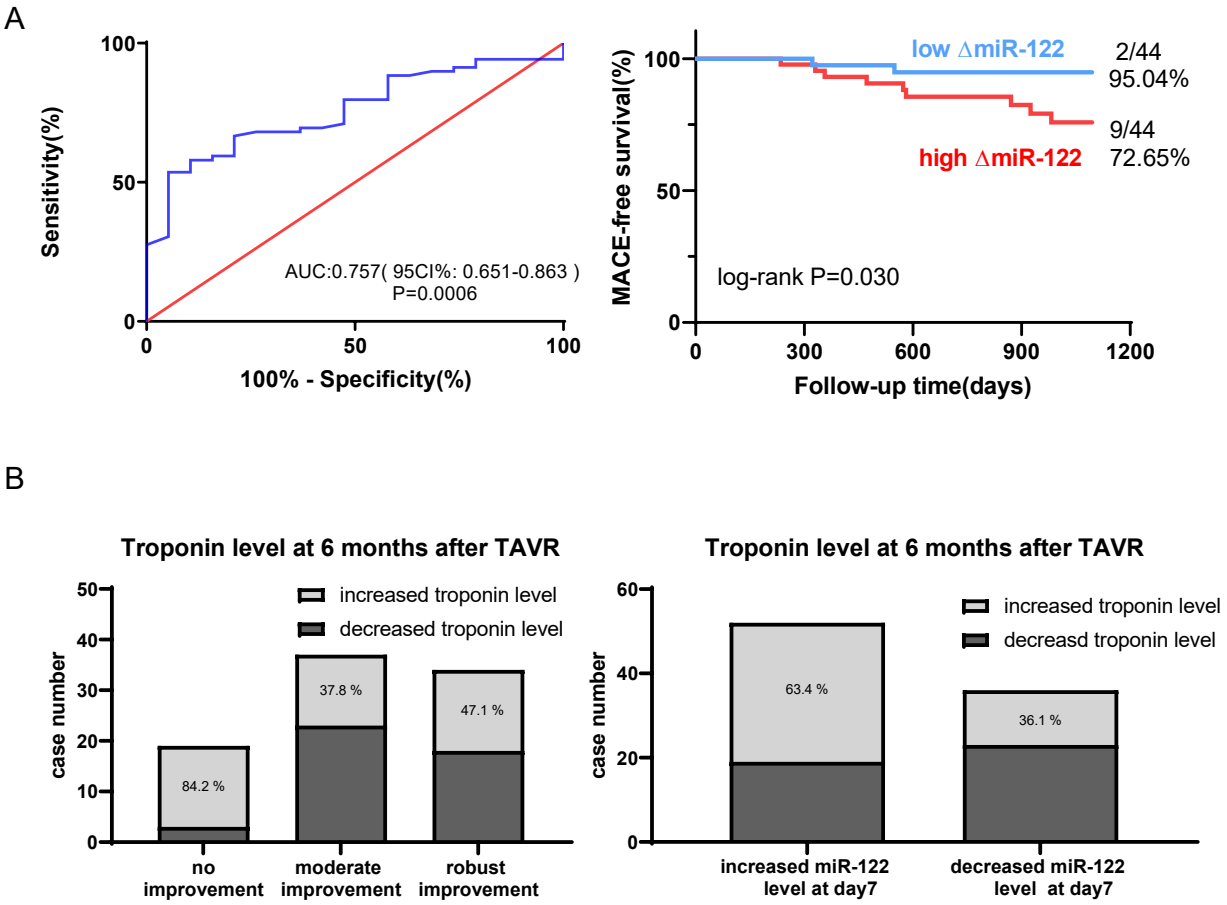

Fig. 7: MiR-122 is associated with clinical outcome after TAVR. (A) Predictive and prognostic value of miR-122. For the predictive value, an ROC curve was used to predict LVEF improvement (>0 %) at 6 months after TAVR by the increase of miR-122 level (day 7 – day -1). For the prognostic value, a Kaplan–Meier survival analysis was applied. MACEs were defined as myocardial infarction, heart failure, cardiac arrest and stroke. Patients were grouped by the median of ΔmiR-122 level (day 7 – day -1). (B) Change of troponin level in different groups of patients. Comparison of the total number of patients with increased troponin level when grouped by LVEF improvement after TAVR (left) and by alteration of miR-122 level (right). A Chi-square test was used for the comparison (p=0.04, p=0.014 respectively).

3.3 Expression and intercelullar transfer of miR-122

Both extracellular vesicles and RNA binding protein stabilize and transport miRs stably in the circulation. To explore in which form (exosomes, MVs or vesicle-free plasma) miR-122 is mainly expressed in plasma, we performed a vesicle-RNA degradation assay. We found that after treatment with Triton X-100, miR-122 was digested significantly by Rnase, but without Triton X-100 treatment the RNA was relatively stable. Triton X-100 disrupted

the phospholipid membrane of vesicles and caused RNAs incorporated within vesicles to lose their protection from RNase (Figure 8A). On the contrary, the sample that was treated with only proteinase K (which digested RNA binding proteins) did not show a significant reduction of miR-122 level. Ultracentrifugation was also performed to separate different size of vesicles and the result confirmed that miR-122 existed mainly in the plasma MVs of patient samples (Figure 8B).

A

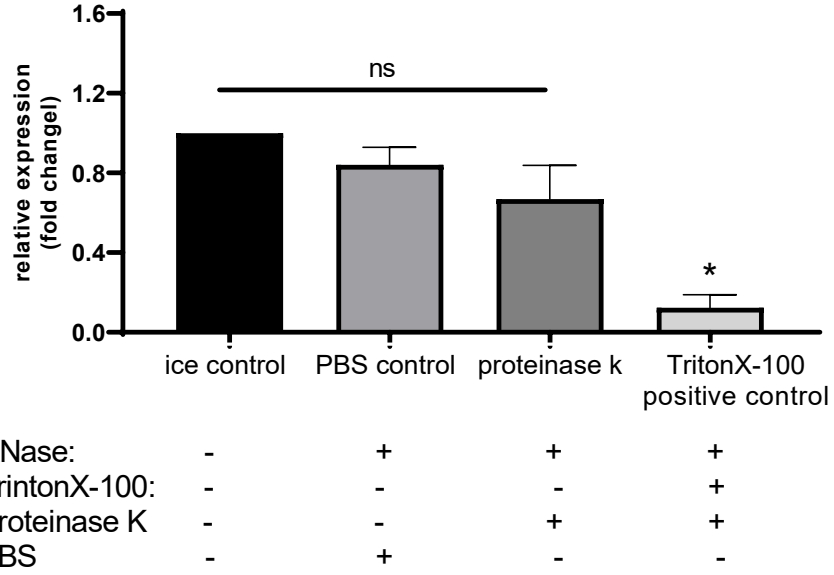

B

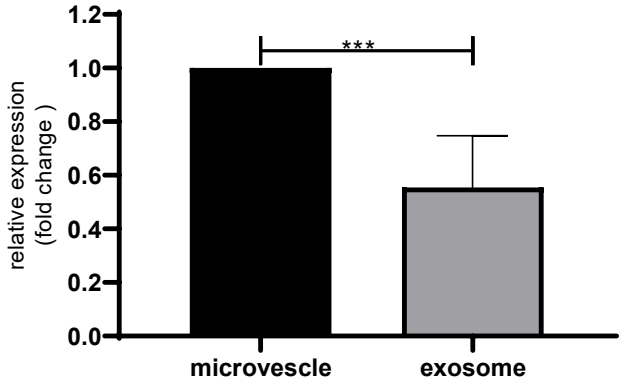

Fig. 8: The expression of miR-122 in plasma. (A) Plasma vesicle-RNA degradation assay. Plasma aliquots were treated in parallel under different conditions, followed by RNAse treatment. MiR-122 was quantified by qRT-PCR and the data are presented as relative expression (*p<0.05, compared with all other groups, n=3, by 1-way ANOVA with Bonferroni correction for multiple comparisons test). (B) MiR-122 expression in plasma compartments. MVs and exosomes were isolated using 20,000xg and 100,000xg centrifugation. MiR-122 was quantified in MV, exosomes by qRT-PCR (***p<0.001, n=6, by 1-way ANOVA). Cel-miR-39 was used as a control.

As MVs were shown to be the primary source of miR-122 in patient plasma and oxidative stress has been shown to actively participate in the pathogenesis of heart failure, we next explored whether oxidative stress, which is common under reduced LVEF conditions, might induce a change in miR-122 expression in MVs from ECs. EC is the most abundant cells in the heart and secrets increased numbers of EVs under oxidative stress condition, we therefore treated ECs with H_2O_2. EC-derived MVs were collected and miR-122 was measured by qRT-PCR. The results showed that miR-122 level increased significantly both in parent ECs and in EC-derived MVs in a dose dependent manner (Figure 9).

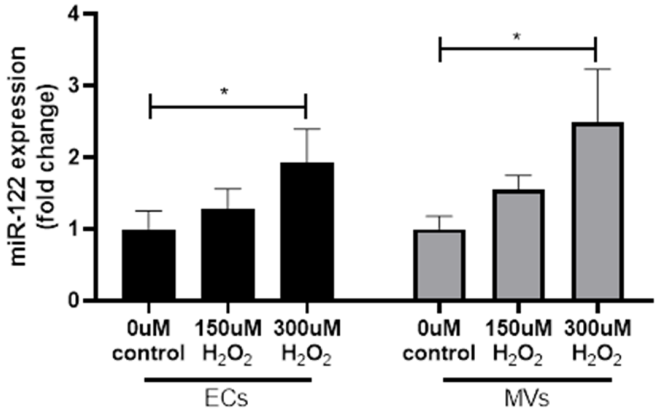

Fig. 9: Oxidative stress increases miR-122 expression in ECs and corresponding MVs. MiR-122 expression was analyzed in ECs and EC-derived MVs after stimulation with different concentrations of H_2O_2 for 24 hours by qRT-PCR (*$p<0.05$, n=3, by 1-way ANOVA with Bonferroni correction for multiple comparisons test. CT values were normalized to Rnu6b and expressed as fold change. H_2O_2, hydrogen peroxide.

Although we have found that miR-122 level was increased in plasma and mostly existed in MVs, it is not yet known whether MVs are an effective vehicle to transfer miR-122 into target cells or not. Therefore, we generated fractions of miR-122 up-regulated EVs in different form (exosomes, MVs) as well as vesicle-free supernatant (containing miRs bound to proteins), followed by incubation of these fractions with target CMs. Interestingly, miR-122 level was much higher in target cells that were incubated with MVs than other groups, which indicates that MVs are highly efficient transporting miR-122 into target cells (Figure 10A). To further demonstrate that miR-122 is directly transfered from donor cells to target cells under physiological conditions, we used fluorescent microscopy to visualize the delivery of endothelial-derived MVs containing miR-122 into target cells, through the

use of fluorescently labeled MVs and miR-122. Co-localization of Cy3-miR-122 (red, miRs) and PKH67 (green, MVs) was observed in the recipient cells (Figure 10B).

A

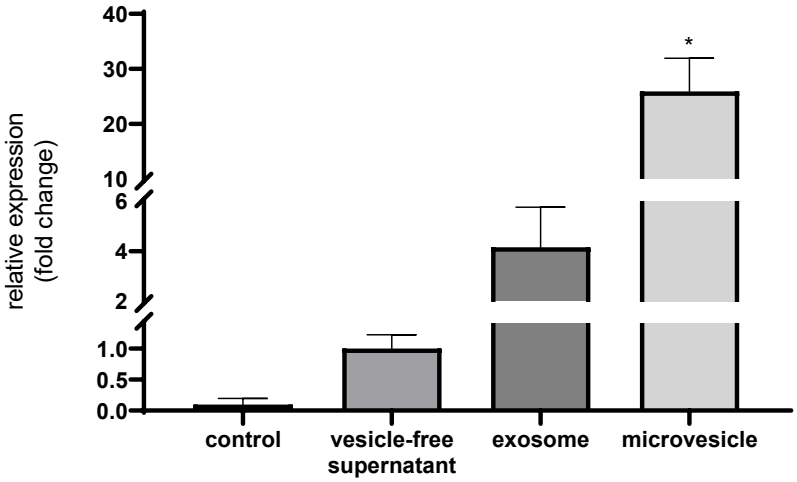

B

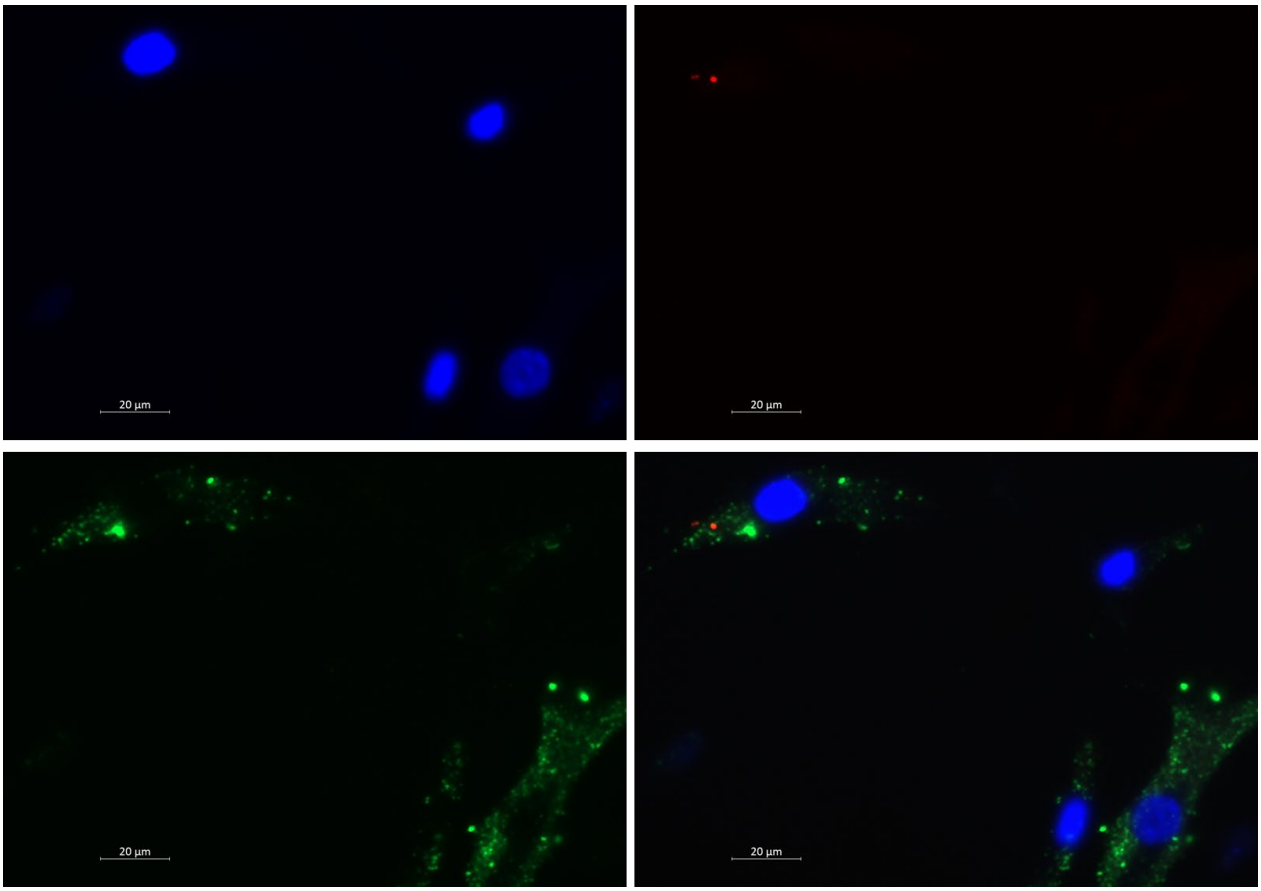

Fig. 10: Intercellular transfer of miR-122. (A) MiR-122 expression was analyzed in recipient CMs after incubation with exosomes, MVs, or vesicle-free supernatant for 24

hous by qRT-PCR (*p<0.05 compared to all other groups, n=6, by 1-way ANOVA with Bonferroni correction for multiple comparisons test). (B) MV-incorporated miR-122 was transferred into recipient CMs. Cy3-labeled miR-122 (red) was transfected into ECs. MVs were derived and labeled with PKH67 (green). Labeled MVs were immediately cultured with recipient CMs for 24 hours. Cell nuclei were stained with DAPI (blue) and the images were taken. Scale bars: 20 μm. Cy3=cyanine 3; DAPI=4′,6-diamidino-2-phenylindole

3.4 MV- incorporated miR-122 regulates cellular function of target cells

Recent studies have demonstrated the extracellular miRs may be implicated in the pathogenesis and modulation of cell functions. As CMs play important roles in maintaining heart function and in heart remodeling, we investigated whether miR-122 can functionally regulate apoptosis of CMs. We performed an apoptosis assay by FACS after transfection of miR-122 (mimic, inhibitor, negative-control scrambled siRNA, or PBS control) into CMs. We found that the rate of apoptosis was higher in the mimic group and lower in the inhibitor group (Figure 11A), meaning that miR-122 has a pro-apoptotic effect. This effect was further confirmed via MTT assay and LDH cytotoxicity assay, in which the miR-122 mimic group showed the lowest viability and highest cytotoxicity ($p<0.05$) (Figure 11B). As miR-122 can be transferred from ECs to CMs via MVs, we further explored the effect of miR-122 incorporated in MV on target CMs. Notably, we obtained similar results following the incubation of MVs containing miR-122 with target CMs. The rate of apoptosis in CMs was higher in MV-miR-122-upregulated group in CMs, which revealed the pro-apoptosis effect of miR-122 on CM via MVs (Figure 12A). An MTT assay also confirmed this effect, showing MV-miR-122-upregulated groups had the lowest cell viability (Figure 12B).

A

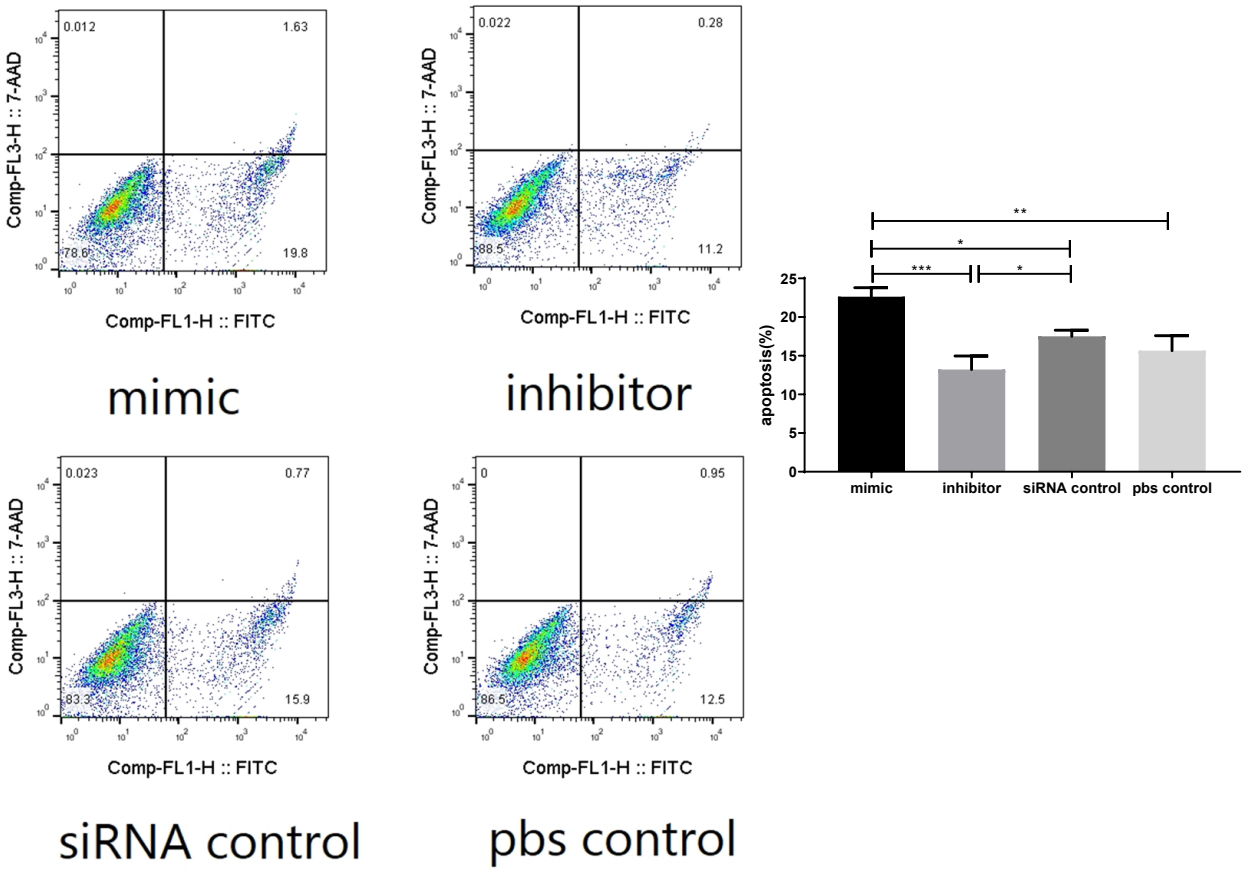

B

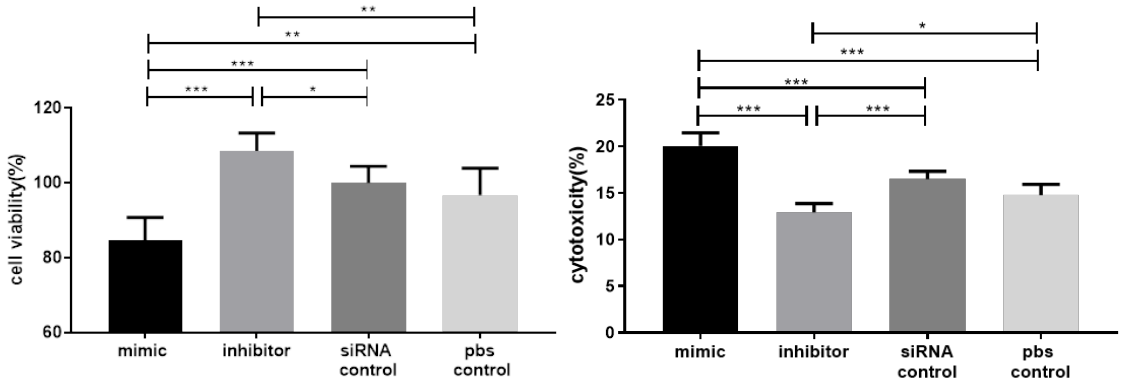

Fig. 11: MiR-122 regulates the function of target CMs. (A) Apoptosis assay of miR-122-transfected CMs by FITC/7-AAD staining. Apoptotic cells were defined as FITC-positive. Data represent the percentage of apoptotic cells and were analyzed by 1-way ANOVA with Bonferroni's multiple comparison test. (*p<0.05, **p<0.01, ***p<0.001, n=3). (B) Cell viability of CMs was measured by using a MTT assay (left) and cell was measured by using an LDH cytotoxicity assay cytotoxicity (right). Data were analyzed by 1-way ANOVA with Bonferroni's multiple comparison test. (*p<0.05, **p<0.01, ***p<0.001).

A

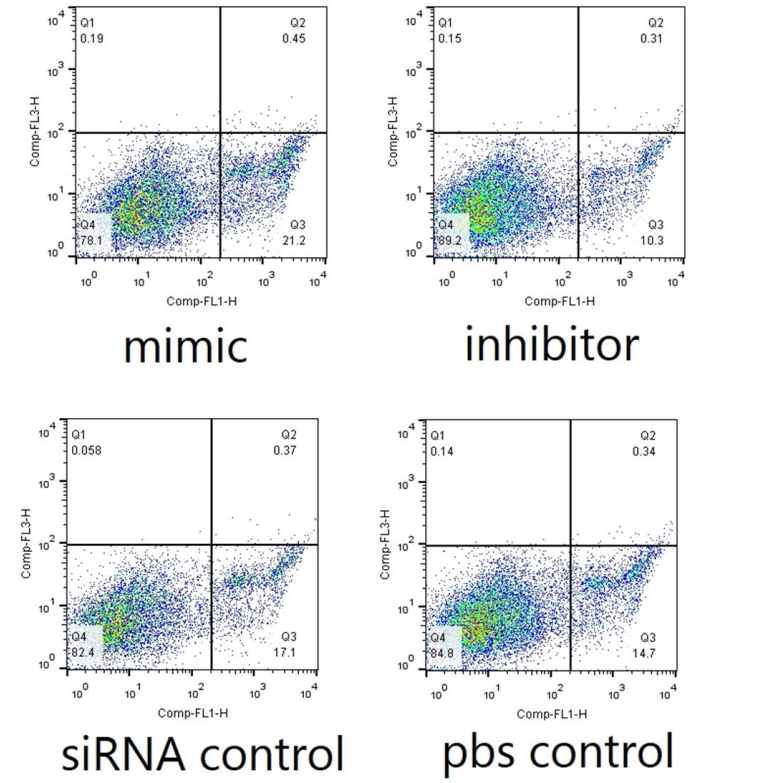

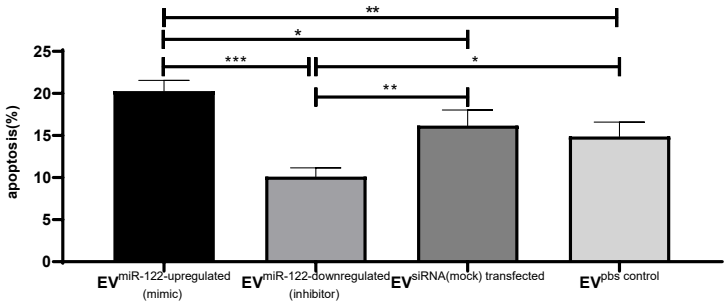

B

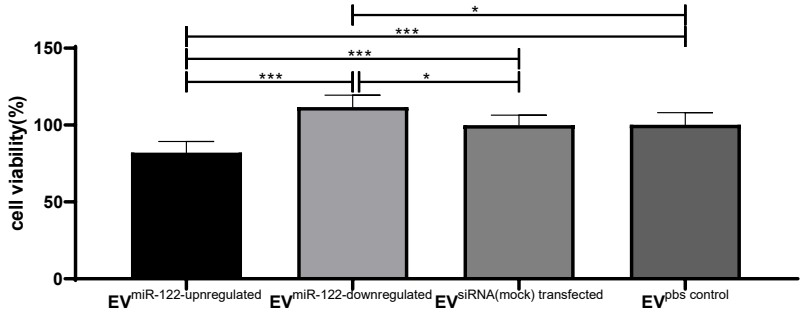

Fig. 12: MiR-122 regulates the function of target CMs via MVs. (A) Apoptosis assay of MV-treated CMs by FITC/7-AAD. Apoptotic cells were defined as FITC-positive. Data represented the percentage of apoptotic cells and were analyzed by 1-way ANOVA with Bonferroni's multiple comparison test. (*p<0.05, **p<0.01, ***p<0.001, n=3). (B) Cell viability of MV-treated CMs were measured by using a MTT assay. Data were analyzed by 1-way ANOVA with Bonferroni's multiple comparison test. (*p<0.05, ***p<0.001).

3.5 MV-mediated transfer of miR-122 regulates recipient CMs by modulating Bcl-2

To further explore the underlying regulatory mechanism of miR-122 in recipient cells, we performed a PCR apoptosis array in miR-122-downregulated CMs and scrambled siRNA control-transfected CMs. Analysis of the array results revealed several genes that were up regulated: Bcl-2($p<0.05$), NOD2($p<0.05$), BIRC8($p=0.17$), NAIP($p=0.12$) (Figure 13). With the identified genes, we further performed qRT-PCR and western blot experiments to confirm the results. We found that only Bcl-2 expression was significantly inhibited by miR-122 upregulation or miR-122-enriched MVs at both mRNA and protein level in CMs (Figure 14A, 14B). Taken together, miR-122 is likely to play a functional role in regulating CM functions by modulating Bcl-2.

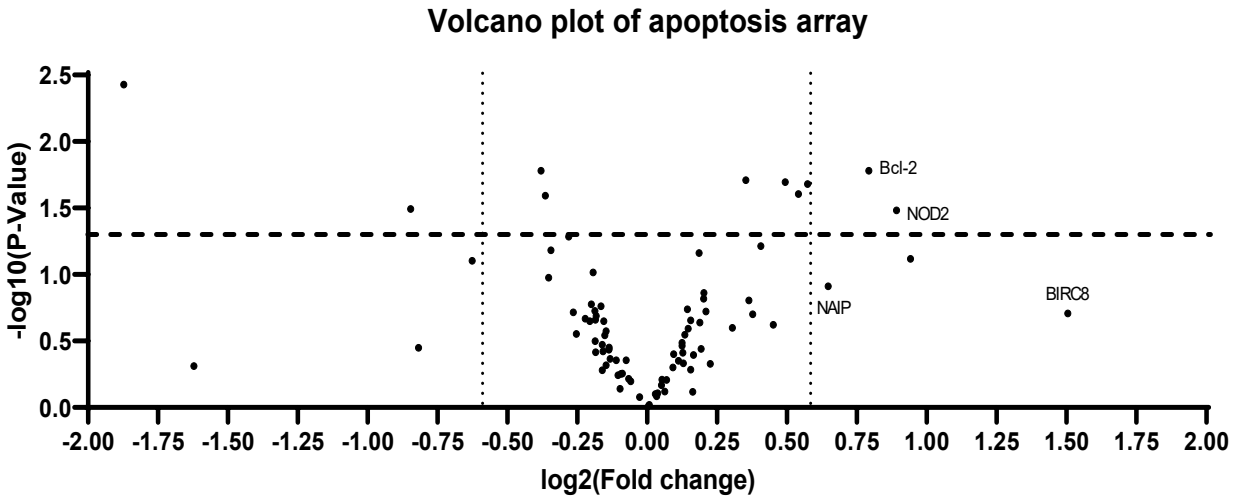

gene	Fold change	P value
Bcl-2	1.732	0.017
NOD2	1.855	0.033
BIRC8	2.837	0.197
NAIP	1.567	0.122

Fig. 13: PCR apoptosis array in recipient CMs after treated with EVs. Apoptosis PCR array of CMs treated with miR-122 inhibitor and a negative control (scrambled siRNA) (n=3). A panel of endogenous controls recommended by the manufacturer were used in the PCR array. Volcano plot and table show the differentially regulated genes. Thresholds of a greater than 1.5-fold difference (vertical lines) and a p-value <0.05 (horizontal line) were applied. Genes with a >1.5-fold change are listed

A

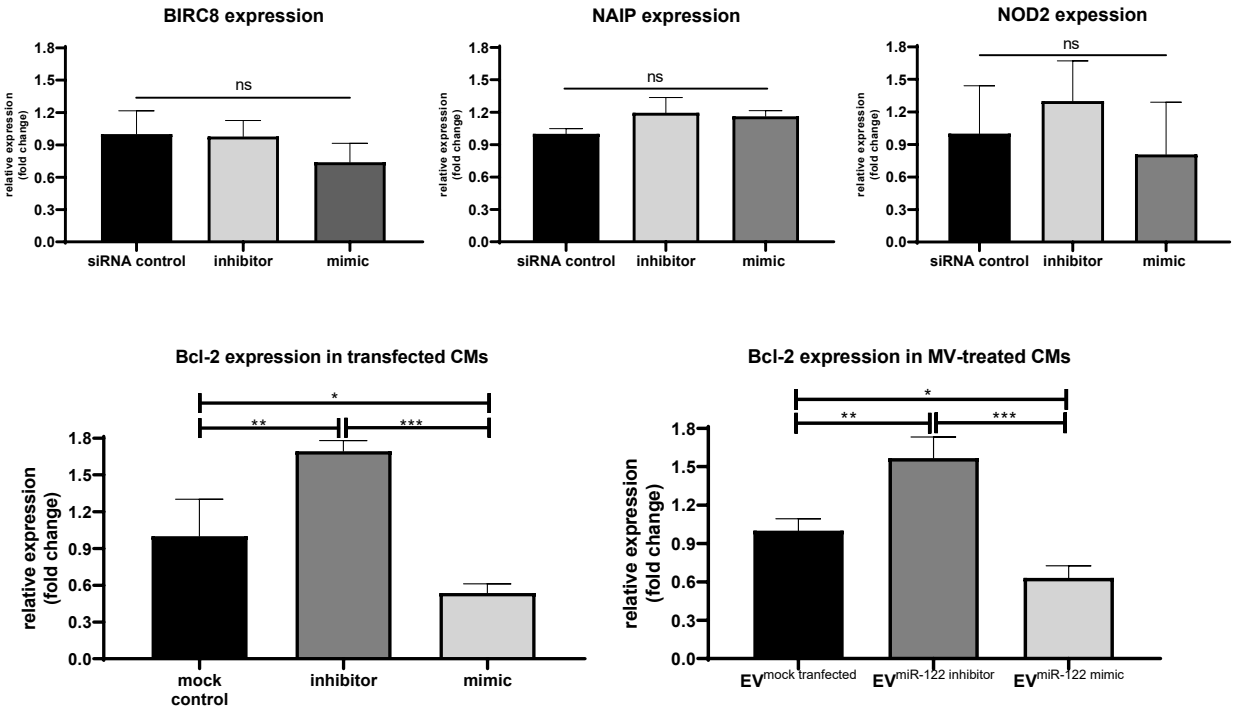

B

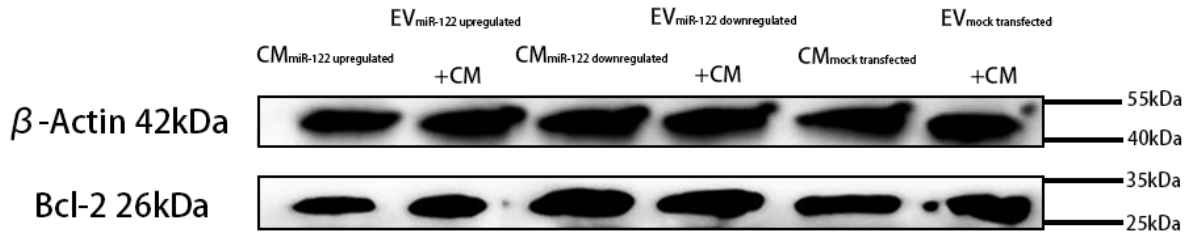

Fig. 14: MV-mediated transfer of miR-122 regulates recipient CMs by modulating Bcl-2. (A) Validation of upregulated genes in CMs. Upper: NAIP, NOD2, BIRC8 expression in CMs that were transfected with miR-122 mimic, inhibitor, or scrambled siRNA was determined by real-time PCR. Bottom left: Bcl-2 expression in CMs that were transfected with miR-122 mimic, inhibitor, or scrambled siRNA. Bottom right: Bcl-2 expression in CMs that were treated with MVs pre-transfected with miR-122mimic, inhibitor, or scrambled siRNA (mock-transfected control). Bcl-2 expression was analyzed by qRT-PCR. (*p<0.05, **p<0.01, ***p<0.001, n=3). (B) Bcl-2 protein expression levels were assessed by western blot. CMs were transfected with miR-122 mimic/inhibitor/scrambled (mock) siRNA. Another group of CMs were incubated with MVs derived from ECs transfected with miR-122 mimic/inhibitor/scrambled (mock) siRNA. β-actin was used as a loading control.

4. Discussion

In this study, we show that plasma miR-122 expression is negatively associated with the improvement of heart function after TAVR in AS patients. Based on our findings from clinical samples, we further described the characteristics of miR-122 regulation and explored the functional role of miR-122. MiR-122 expression was higher in patients with low LVEF and was found to be released into the circulation mostly in the vesicle-bound form. Oxidative stress induced miR-122 elevation in MVs, which were shown to be effectively taken up by CMs. *In vitro*, miR-122 induced apoptosis of CMs via MVs. We showed that this effect was related to the regulation of gene Bcl-2.

In patients with aortic stenosis, the low left ventricular ejection fraction indicates the severity of the pathological changes in the failing heart and the urgency of replacing the valve to relieve symptom and reduce the burden on the heart. However, some of these patients do not develop an improved LVEF after TAVR. So far, it has not been widely investigated what biological or physiological differences there might be in this group of AS patients. Within the field of cardiovascular research, a wide range of studies has reported on the dynamic alterations of circulating miRNA expression with regard to various cardiovascular conditions, both physiological and pathologic, leading to a rising interest in these values for clinical diagnosis and prognosis (Pleister, et al., 2013).

Therefore, we compared the miR level of patients with different response to TAVR after a six-month follow-up. Interestingly, the result of our microarray result did not identify several widely investigated miRs in cardiovascular diseases, such as miR-1, miR-133, miR-208, which have been associated with heart failure and myocardial infarction. In our study, after qRT- PCR validation, we discovered that miR-122 could be the potential biomarker. Patients with robust LVEF improvement at six months had a lower miR-122 level after TAVR compared to patients with no LVEF improvement. There was a negative correlation between LVEF improvement and increasing of miR-122 level from day 7 plasma, which indicates that a stronger elevation of miR-122 level after TAVR could predict a worse outcome (no or little LVEF improvement). Several studies have demonstrated that in patients with heart failure, the miR-122 level is higher than in healthy subjects (Stefan, et al., 2013, Vogel, et al., 2013, Corsten, et al., 2010). This is in line with

our result that AS patients with low LVEF have a higher level of miR-122 expression than those patients with higher LVEF. These results also indicate that an elevation of miR-122 levels could be a marker when heart function deteriorated.

Next, we further explored the distribution of miR-122. As described above, miRs can be released into the circulation via different carriers. Some of miRs are released in a free circulating form. They are unstable, vulnerable to enzyme and will be digested in the blood. However, some other miRs are EV-bound and the bilayer membrane of EVs could protect the miRs from enzymatic degradation. We therefore performed a vesicle-RNA degradation assay as well as ultracentrifugation and conformed that miR-122 is mainly expressed in MVs under pathological condition. Besides this, we explored if oxidative stress, a factor significantly related to heart failure, could induce the upregulation of miR-122 in MVs in a dose-dependent manner. In recent investigations, EVs have been proved to play a crucial role in intercellular signaling and regulation of cellular function. Once released, EVs can target both neighboring and distant recipient cells and can be internalized via ligand/receptor signaling and/or fusion of the vesicle with the plasma membrane of the recipient cells. During this process, bioactive cargo from the EVs can enter the cytoplasm or nucleus of the cell, thus influencing the function and phenotype of the EV-recipient cells. EVs can transfer proteins, cytokines, mRNAs, and non-coding RNAs to target cells to influence their behavior. Because they transfer biological messages between cells, EVs are emerging as crucial regulators of the progression of cardiovascular disease. Previous studies indicated that cells can selectively package miRs into MV and these miRs act as signaling molecules to mediate cell-cell communication (Liu, et al., 2019, Jansen, et al., 2013). We isolated exosomes, MVs and vesicle-free supernatant from the ECs medium and incubated them with target cells. Intriguingly, MVs mediated transfer was the most effective way to transfer miR-122 into target cells. The transfer of MVs was also directly confirmed by fluorescence microscopy. MiR-122 has previously been shown to be highly expressed in liver. Originally, miR-122 was reported as a tumor suppressor gene in hepatocellular carcinoma (Gramantieri, et al., 2007). However, many studies have investigated the presence and functional role of miR-122 in other tissues and cells. MiR-122 regulates cutaneous T cell lymphoma through the p53/Akt signaling pathway and promotes renal cancer-cell proliferation by targeting

Sprouty2 (Manfe, et al., 2012, Wang, et al., 2017). It has also been implicated in the regulation of fatty acid metabolism (Fernández, et al., 2011). More recently, evidence has revealed an increased expression of miR-122 in a rat model of post-infarction heart failure (Xueyan, et al., 2016). CMs isolated from mice with atrial fibrillation expressed more miR-122 than control mice (Xiangqun, et al., 2018). Additionally, another study demonstrated that in heart failure patients, the miR-122 level in the coronary sinus is significantly higher than peripheral arterial blood, which suggests that miR-122 is released from the heart under heart failure conditions (Francine, et al., 2016).

As previously described, miR-122 expression can be altered in the heart tissue in response to different stimuli. In heart failure patients with aortic stenosis, a reduction in the density of cardiac capillary and tissue hypoxia leads to cell death and interstitial fibrosis and further contributes to contractile dysfunction and heart failure. Therefore, we focused on the regulatory role of miR-122 in CMs. We observed a higher percentage of apoptotic cells when the expression of miR-122 was upregulated by transfection or incubation with miR-122 containing vesicle. This is in line with several publications revealing the apoptotic effect of miR-122 (Zhang, et al., 2018, Wang, et al., 2018). A further mechanism was investigated by using PCR-based gene expression array. Our results indicated that anti-apoptotic B cell lymphoma 2 (Bcl-2) was effectively regulated in CMs in response to miR-122 regulation, which was verified at mRNA level.

Unitil now, many miRNAs have been identified to target Bcl-2 or have negative correlation with the expression of BCL2 family members (Cui, et al., 2018). Bcl-2 family members (Bcl-2, Mcl-1, Bcl-xL, Bcl-W, and Bfl1) are key players in the regulation of intrinsic apoptosis. They control apoptosis by regulation of outer mitochondrial membrane permeabilization. Dysregulation of these proteins could impair normal development and contributes to tumor progression. Therefore, the expression of Bcl-2 family members is under strict control using multiple mechanisms to maintain normal cell function. It has also become evident that the Bcl-2 family proteins play a central role in regulating apoptosis in the cardiovascular system (Gustafsson, et al., 2007). Antiapoptotic Bcl-2 proteins are expressed in the myocardium during development and in adult hearts. In the human heart, the level of antiapoptotic Bcl-2 proteins has been shown to be down-regulated in various pathological processes such as myocardial infarction, dilated cardiomyopathy, and

ischemic heart disease. Bcl-2 family proteins have been proved to affect many mechanisms of cardiac damage, including ischemia, calcium dysregulation, and oxidative stress. Of note, from a previous publication, Bcl-2 family proteins were downregulated in myocytes exposed to 0.2 mM H_2O_2. Because H_2O_2 stimulation can elevate the level of miR-122, it is likely that miR-122 could be one of mediators for H_2O_2 to inhibit expression of Bcl-2 famly members (Donna et al., 2003)

However, there are some limitations to our study that should be mentioned. (i) As we only have plasma samples that were obtained during the TAVR procedure (day -1 to day 7), the miR-122 level at a later timepoint, such as six months (consistent with echocardiography parameters) is unknown, which could affect the accuracy of the association (ii) Although we specifically transfected miR-122 to generate MVs, it is still technically challenging to keep the complete contents of vesicles equal, which could affect the results of the downstream experiments. (iii) A further animal model that could mimic the afterload reduction in AS animal needs to be established. This would help to understand the mechanisms occuring in patients with no LVEF improvement.

5. Summary

Transcatheter aortic valve replacement is an established treatment for aortic stenosis patients. However, some patients fail to develop an improvement in LVEF after TAVR. MiRs are novel biomarkers and regulators of cardiovascular disease. We aimed to explore whether circulating miRs are differently modulated in patients with different response to TAVR.

96 AS patients with impaired LVEF (<45 %) were divided into three groups according to their LVEF improvement, assessed after six months. Taqman miR array was performed in the groups of patients with no LVEF improvement and >15 % LVEF improvement. Twelve miRs were differently expressed in the discovery cohort but only miR-122 expression was significantly elevated after validation. The increase of miR-122 level was negatively associated with LVEF improvement. *In vitro*, treatment with H_20_2 increased miR-122 level in endothelial-derived MVs. A vesicle RNA degradation experiment and separation by ultracentrifugation showed that miR-122 was mainly incorporated in MVs. Confocal microscopy confirmed the fluroscently-labeled MVs were taken up by CMs. Gain- and loss-of-function experiments indicated that miR-122 can induce apoptosis of recipient CMs via the transfer of MVs. Up- or down-regulation of miR-122 results in a corresponding alteration of Bcl-2 expression at mRNA level.

In summary, changes in the circulating level of pro-apoptotic miR-122 significantly correlate with LVEF improvement after TAVR in low LVEF patients. MVs can mediate the transfer of miR-122 into target CMs and further influence their biological functions.

6. List of Figures

7. List of Tables

8. References

Arroyo JD, Chevillet JR, Kroh EM, Ruf IK, Pritchard CC, Gibson DF, Mitchell PS, Bennett CF, Pogosova-Agadjanyan EL, Stirewalt DL. Argonaute2 complexes carry a population of circulating microRNAs independent of vesicles in human plasma. Proc Natl Acad Sci U S A 2011; 108: 5003-5008

Badeer HS. Biological significance of cardiac hypertrophy. Am J Cardiol 1964; 14: 133-138

Bang C, Batkai S, Dangwal S, Gupta SK, Foinquinos A, Holzmann A. Cardiac fibroblast-derived microRNA passenger strand-enriched exosomes mediate cardiomyocyte hypertrophy. J Clin Invest 2014; 124: 2136-2146

Barwari T, Joshi A, Mayr M. MicroRNAs in cardiovascular disease. J Am Coll Cardiol 2016; 68: 2577-2584

Carabello BA, Paulus WJ. Aortic stenosis. Lancet 2009; 373: 956-966

Corsten MF, Dennert R, Jochems S, Kuznetsova T, Devaux Y, Hofstra L, Wagner DR, Staessen JA, Heymans S and Schroen B. Circulating microRNA-208b and microRNA-499 reflect myocardial damage in cardiovascular disease. Circ Cardiovasc Genet 2010; 3: 499-506

Cui J, Placzek WJ. Post-transcriptional regulation of anti-Apoptotic BCL2 family members. Int J Mol Sci 2018; 19: 308

Cully M. Exosome-based candidates move into the clinic. Nat Rev Drug Discov 2021; 20: 6-7

Fearon U, Reece R, Smith J, Emery P, Veale DJ. Synovial cytokine and growth factor regulation of MMPs/TIMPs: implications for erosions and angiogenesis in early rheumatoid and psoriatic arthritis patients. Ann NY Acad Sci 1999; 878: 619-621

Gan L, Xie D, Liu J, Lau WB, Christopher TA, Lopez B, Zhang L, Gao E, Koch W, Ma XL, Wang YJ. Small extracellular microvesicles mediated pathological communications between dysfunctional adipocytes and cardiomyocytes as a novel mechanisms exacerbating ischemia/reperfusion injury in diabetic. Circulation 2020; 141: 968-983

Gleason TG, Reardon MJ, Popma JJ, Deeb GM, Yakubov SJ, Lee JS, Kleiman NS, Chetcuti S, Hermiller JB, Heiser J, Merhi W, Zorn GL, Tadros P, Robinson N, Petrossian G, Hughes GC, Harrison JK, Conte JV, Mumtaz M, Oh JK, Huang J, Adams DH, CoreValve U.S. Pivotal High Risk Trial Clinical Investigators. 5-Year outcomes of self-expanding transcatheter versus surgical aortic valve replacement in high-risk patients. J Am Coll Cardiol 2018; 72: 2687-2696

Gramantieri L, Ferracin M, Fornari F, Veronese A, Sabbioni S, Liu CG, Calin GA, Giovannini C, Ferrazzi E, Grazi GL. Cyclin G1 is a target of miR-122a, a microRNA frequently down-regulated in human hepatocellular carcinoma. Cancer Res 2007; 67: 6092-6099

Gupta SK, Foinquinos A, Thum S, Remke J, Zimmer K, Bauters C. Preclinical development of a microRNA-based therapy for elderly patients with myocardial infarction. J Am Coll Cardiol 2016; 68: 1557-1571

Gustafsson AB, Gottlieb RA. Bcl-2 family members and apoptosis, taken to heart. Am J Physiol Cell Physiol 2007; 292: C45-51

Hein S, Arnon E, Kostin S, Schönburg M, Elsässer A, Polyakova V, Bauer EP, Klövekorn WP, Schaper J. Progression from compensated hypertrophy to failure in the pressure overloaded human heart: structural deterioration and compensatory mechanisms. Circulation 2003; 107: 984-991

Hernando CF, Suárez Y, Rayner KJ, Moore KJ. MicroRNAs in lipid metabolism. Curr Opin Lipidol 2011; 22: 86-92

Herrmann HC., Han YC. Identifying patients who do not benefit from transcatheter aortic valve replacement. Circ Cardiovasc Interv 2014; 7: 136-138

Hosen MR, Goody PR, Zietzer A, Nickenig G, Jansen F. MicroRNAs as master regulators of atherosclerosis: from pathogenesis to novel therapeutic options. Antioxid Redox Signal 2020; 33: 621-644

Howard C. Herrmann, Yuchi Han. Identifying Patients Who Do Not Benefit From Transcatheter Aortic Valve Replacement. Circ Cardiovasc Interv 2014; 7: 136-138

Howard CM, Baudino TA. Dynamic cell-cell and cell-ECM interactions in the heart. J Mol Cell Cardiol 2014; 70: 19-26

Hunter MP, Ismail N, Zhang X, Aguda BD, Lee EJ, Yu L, Xiao T, Schafer J, Lee M-LT, Schmittgen TD, Nana-Sinkam SP, Jarjoura D, Marsh CB. Detection of microRNA expression in human peripheral blood microvesicles. PLoS One 2008; 3: e3694

Jansen F, Wang H, Przybilla D, Franklin BS, Dolf A, Pfeifer P, Schmitz T, Flender A, Endl E, Nickenig G. Vascular endothelial microparticles-incorporated microRNAs are altered in patients with diabetes mellitus. Cardiovasc Diabetol 2016; 15: 49

Jansen F, Yang X, Hoelscher M, Cattelan A, Schmitz T, Proebsting S, Wenzel D, Vosen S, Franklin BS, Fleischmann BK. Endothelial microparticle-mediated transfer of MicroRNA-126 promotes vascular endothelial cell repair via SPRED1 and is abrogated in glucose-damaged endothelial microparticles. Circulation 2013; 18: 2026-2038

Lambert E, Dassé E, Haye B, Petitfrère E. TIMPs as multifacial proteins. Crit Rev Oncol/Hemat 2004; 49: 187-198

Liu XY, Meng H, Jiang C, Yang S, Cui F, Yang P. Differential microRNA expression and regulation in the rat model of post infarction heart failure. PLoS One 2016; 11: e0160920

Liu YY, Li Q, Hosen MR, Zietzer A, Flender A, Levermann P, Schmitz T, Frühwald D, Goody P, Nickenig G, Werner N, Jansen F. Atherosclerotic conditions promote the packaging of functional microRNA-92a-3p into endothelial microvesicles. Circ Res 2019; 124: 575-587

Manfe V, Biskup E, Rosbjerg A, Kamstrup M, Skov AG, Lerche CM, Lauenborg BT, Odum N, Gniadecki R. MiR-122 Regulates p53/Akt signaling and the chemotherapy-induced apoptosis in cutaneous T-Cell lymphoma. PLoS One 2012; 7: e29541

Marques FZ, Vizi D, Khammy O, Mariani JA, Kaye DM. The transcardiac gradient of cardio-microRNAs in the failing heart. Eur J Heart Fail 2016; 18: 1000-1008

Melman YF, Shah R, Danielson K, Xiao JJ, Simonson B, Barth A, Chakir K, Lewis GD, Lavender Z, Truong QA, Kleber A, Das R, Rosenzweig A, Wang YY, Kass DA, Singh JP, Das S. Circulating microRNA-30d is associated with response to cardiac resynchronization therapy in heart failure and regulates cardiomyocyte apoptosis-a translational pilot study. Circulation 2015; 131: 2202-2216

Midgley AC, Rogers M, Hallett MB, Clayton A, Bowen T, Phillips AO. Transforming growth factor-β1 (TGF-β1)-stimulated fibroblast to myofibroblast differentiation is mediated by hyaluronan (HA)-facilitated epidermal growth factor receptor (EGFR) and CD44 co-localization in lipid rafts. J Biol Chem; 2013. 288: 14824-14838

Nishimura RA, Otto CM, Bonow RO. 2014 AHA/ACC guideline for the management of patients with valvular heart disease: a report of the american college of cardiology/american heart association task force on practice guidelines. J Am Coll Cardiol 2014; 63: 2438-2488

Ovchinnikova ES, Schmitter D, Vegter EL, Ter Maaten JM, Valente MA, Liu LC. Signature of circulating microRNAs in patients with acute heart failure. Eur J Heart Fail 2016; 18: 414-423

Paulus WJ, Tschope C. A novel paradigm for heart failure with preserved ejection fraction: comorbidities drive myocardial dysfunction and remodeling through coronary microvascular endothelial inflammation. J Am Coll Cardiol 2013; 62: 263-271

Pinto AR, Ilinykh A, Ivey MJ, Kuwabara JT, D'Antoni ML, Debuque R, Chandran A, Wang L, Arora K, Rosenthal N, Tallquist MD. Revisiting cardiac cellular composition. Circ Res 2016; 118: 400-409

Pleister A, Selemon H, Elton SM, Elton TS. Circulating miRNAs: novel biomarkers of acute coronary syndrome? Biomark Med 2013; 7: 287-305

Rychli K, Kaun C, Hohensinner PJ. The anti-angiogenic factor PEDF is present in the human heart and is regulated by anoxia in cardiac myocytes and fibroblasts. J Cell Mol Med 2010; 14: 198-205

Salcedo R, Ponce ML, Young HA, Wasserman K, Ward JM, Kleinman HK, Oppenheim JJ, Murphy WJ. Human endothelial cells express CCR2 and respond to MCP-1: direct role of MCP-1 in angiogenesis and tumor progression. Blood 2000; 96: 34-40

Sawyer DB, Siwik DA, Xiao L, Pimentel DR, Singh K, Colucci WS. Role of oxidative stress in myocardial hypertrophy and failure. J Mol Cell Cardiol 2002; 34: 379-388

Segers VF, Lee RT. Stem-cell therapy for cardiac disease. Nature 2008; 451: 937-942

Stamatovic SM, Keep RF, Mostarica-Stojkovic M, Andjelkovic AV. CCL2 Regulates Angiogenesis via Activation of Ets-1 Transcription Factor. J Immunol 2006; 177: 2651-2661

Stojkovica S, Kollera L, Sulzgrubera P. Liver-specific microRNA-122 as prognostic biomarker in patients with chronic systolic heart failure. Int J Cardiol 2020; 303: 80-85

Tijsen AJ, Creemers EE, Moerland PD, de Windt LJ, van der Wal AC, Kok WE, Pinto YM. MiR423-5p as a circulating biomarker for heart failure. Circ Res. 2010;106:1035–1039

Thompson SA, Copeland CR, Reich DH, Tung L. Mechanical coupling between myofibroblasts and cardiomyocytes slows electric conduction in fibrotic cell monolayers. Circulation 2011; 123: 2083-2093

Thyregod HG, Ihlemann N, Jørgensen TH, Nissen H, Kjeldsen BJ, Petursson P, Chang Y, Franzen OW, Engstrøm T, Clemenssen P, Hansen PB, Andersen LW, Steinbrüchel DA, Olsen PS, Søndergaard L. Five-year clinical and echocardiographic outcomes from the Nordic Aortic Valve Intervention NOTION randomized clinical trial in patients at lower surgical risk. Circulation 2019; 139: 2714-2723

Tsui NB, Ng EK, Lo YM. Stability of endogenous and added RNA in blood specimens, serum, and plasma. Clin Chem 2002; 48: 1647-1653

Turchinovich A, Weiz L, Langheinz A, Burwinkel B. Characterization of extracellular circulating microRNA. Nucleic Acids Res 2011; 39: 7223-7233

Valks DM, Kemp TJ, Clerk A. Regulation of Bcl-xL expression by H_2O_2 in cardiac mocytes. J Biol Chem 2003; 278: 25542-25547.

Villari B, Vassalli G, Monrad ES. Normalization of diastolic dysfunction in aortic stenosis late after valve replacement. Circulation 1995; 91: 2353–2358

Vincent F. M. Segers, Dirk L. Brutsaert, Gilles W. De Keulenaer. Cardiac remodeling: endothelial cells have more to say than just NO. Front Physiol 2018; 9: 382

Vogel B, Keller A, Frese KS, Leidinger P, Hamedani FS, Kayvanpour E, Kloos W, Backe C, Thanaraj A, Brefort T, Beier M, Hardt S, Meese E, Katus HA, Meder B. Multivariate miRNA signatures as biomarkers for non-ischaemic systolic heart failure. Eur Heart J 2013; 34: 2812-2822

Wang XT, Yang CY, Liu XY, Yang P. The impact of microRNA-122 and its target gene Sestrin-2 on the protective effect of ghrelin in angiotensin II-induced cardiomyocyte apoptosis. RSC Adv 2018; 8: 10107-10114

Wang Z, Qin C, Zhang J, Han ZJ, Tao J, Cao Q, Zhou WL, Xu Z, Zhao CC, Tan RY, Gu M. MiR-122 promotes renal cancer cell proliferation by targeting Sprouty2. Tumour Biol 2017; 39: 1010428317691184

Yu X, Deng LY, Wang D, Li N, Chen X, Cheng X, Yuan J, Gao XL, Liao MY, Wang M, Liao YH. Mechanism of tnf-alpha autocrine effects in hypoxic cardiomyocytes: Initiated by hypoxia inducible factor 1 alpha, presented by exosomes. J Mol Cell Cardiol 2012; 53: 848-857.

Yutzey KE, Demer LL, Body SC, Huggins GS, Towler DA, Giachelli CM, Hofmann-Bowman MA, Mortlock DP, Rogers MB, Sadeghi MM, Aikawa E. Calcific aortic valve

disease-a consensus summary from the alliance of investigators on calcific aortic valve disease. Arterioscler Thromb Vasc Biol 2014; 34: 2387-2393

Zaborowski MP, Balaj L, Breakefield XO, Lai CP. Extracellular vesicles: composition, biological relevance and methods of study. Bioscience 2015; 65: 783-797

Zhang XQ, Jing WL. Upregulation of miR‐122 is associated with cardiomyocyte apoptosis in atrial fibrillation. Mol Med Rep 2018; 18: 1745-1751

Zhang Y, Liu YJ, Liu T, Zhang H, Yang SJ. Plasma microRNA-21 is a potential diagnostic biomarker of acute myocardial infarction. Eur Rev Med Pharmacol Sci 2016; 20: 323-329

9. Acknowledgments

I would like to thank all those who helped me during the study in Bonn and the writing of this thesis.

First and foremost, I wish to express gratitude to my supervisor PD. Dr. med. Felix Jansen. I gratefully acknowledge the help of his supervision and his valuable suggestions during the process of my research.

Second, I gratefully acknowledge the help of Prof. Dr. med. Nikos Werner, who has offered me a chance to study in this great research group and gave me a lot of support.

Third, I give my great appreciation to the post-doctoral fellow who was my mentor for this project, Dr. rer. nat. Mohammed Rabiul Hosen. He is a very supportive, cheerful, and energetic researcher and gave me lots of helpful information and insightful advice at every steps of my thesis.

I am also grateful to all the colleagues in the lab who have helped me with my research. I must express my thanks to Dr. med. Philip R. Goody, Dr. med. Andreas Zietzer, Ms. Anna Flender, Ms. Paula Levermann, Ms. Theresa Schmitz and Ms. Sarah Arahouan for their assistance.

I would like to thank also Chinese scholarship committee for their financial support, which has made my project in Germany possible.

Last but not least, I would like to express my special thanks to my beloved parents, I will always be grateful for their love.